Supplementary Material

The content includes the supplementary figures, tables, and algorithms.

Contents

Fig. S1: Visualization of the detailed evaluation of the AirMorph on subsegmental bronchi. TLD is reported. AirwayNet is compared with UNet and nnUNet.

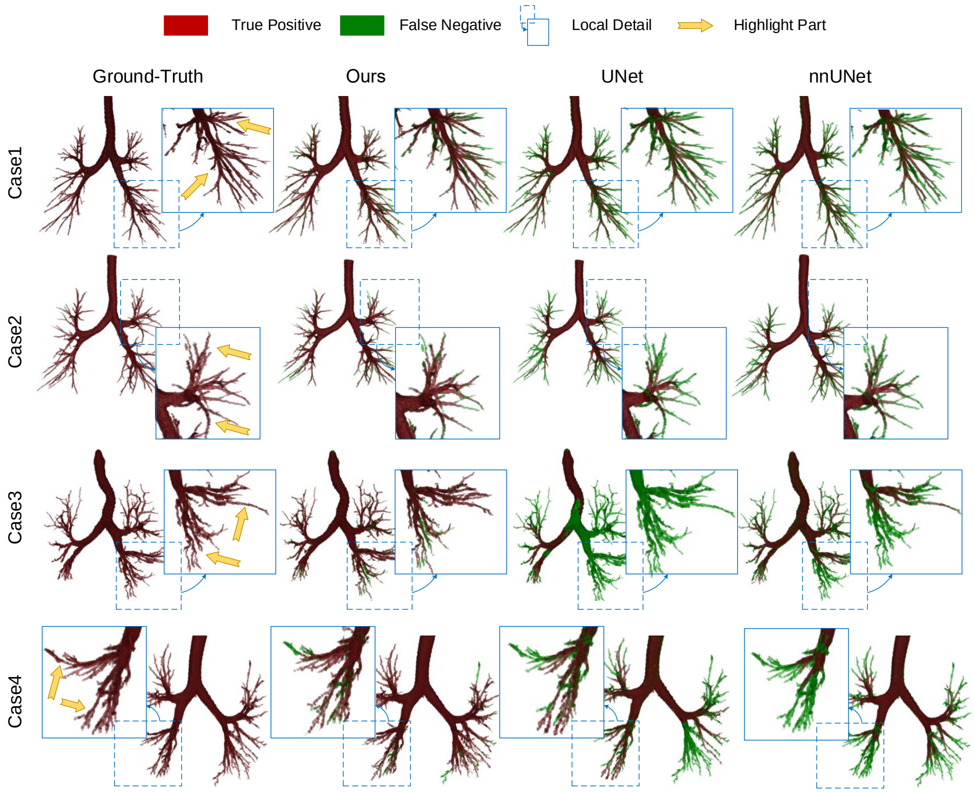

Fig. S2: Visualization of the quantitative comparison of the binary airway modeling. Case 1 and Case 2 are from the ATM'22 Dataset, Case 3 and Case 4 are from AIIB'23 Dataset.

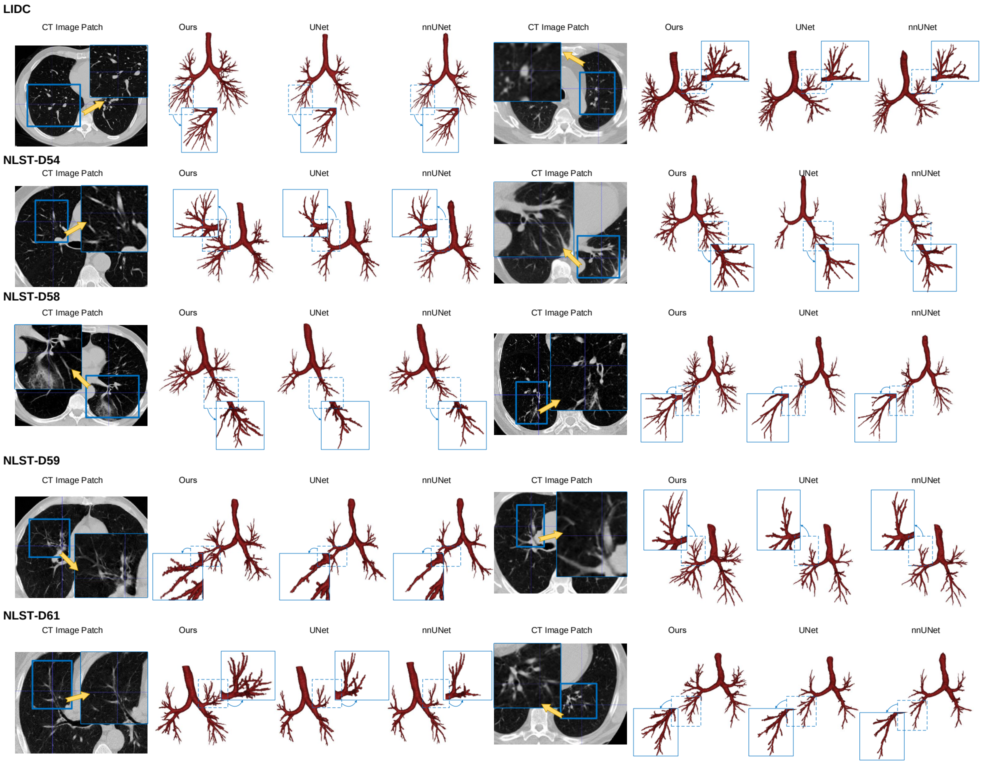

Fig. S3: Visualization of the qualitative comparison of the binary airway modeling.

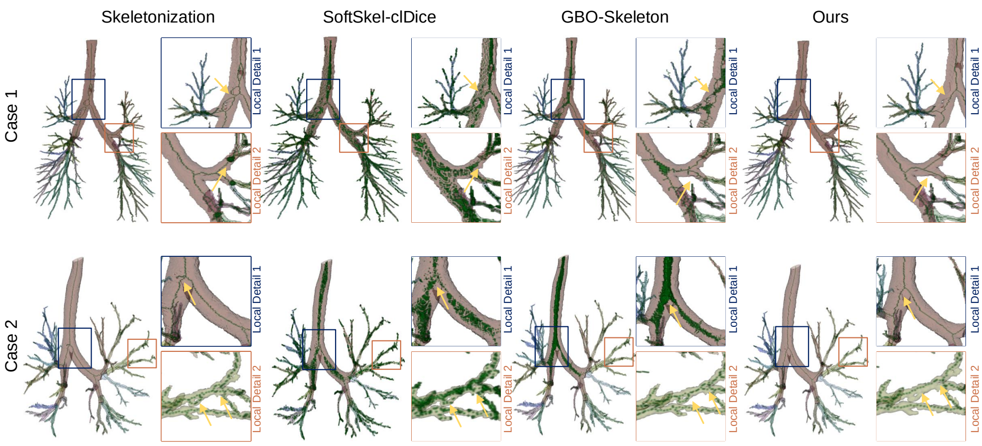

Fig. S4: Comparison of graph construction strategies for feature extraction in airway anatomical labeling. Case1 and Case2 are selected from ATM'22 and AIIB'23, respectively.

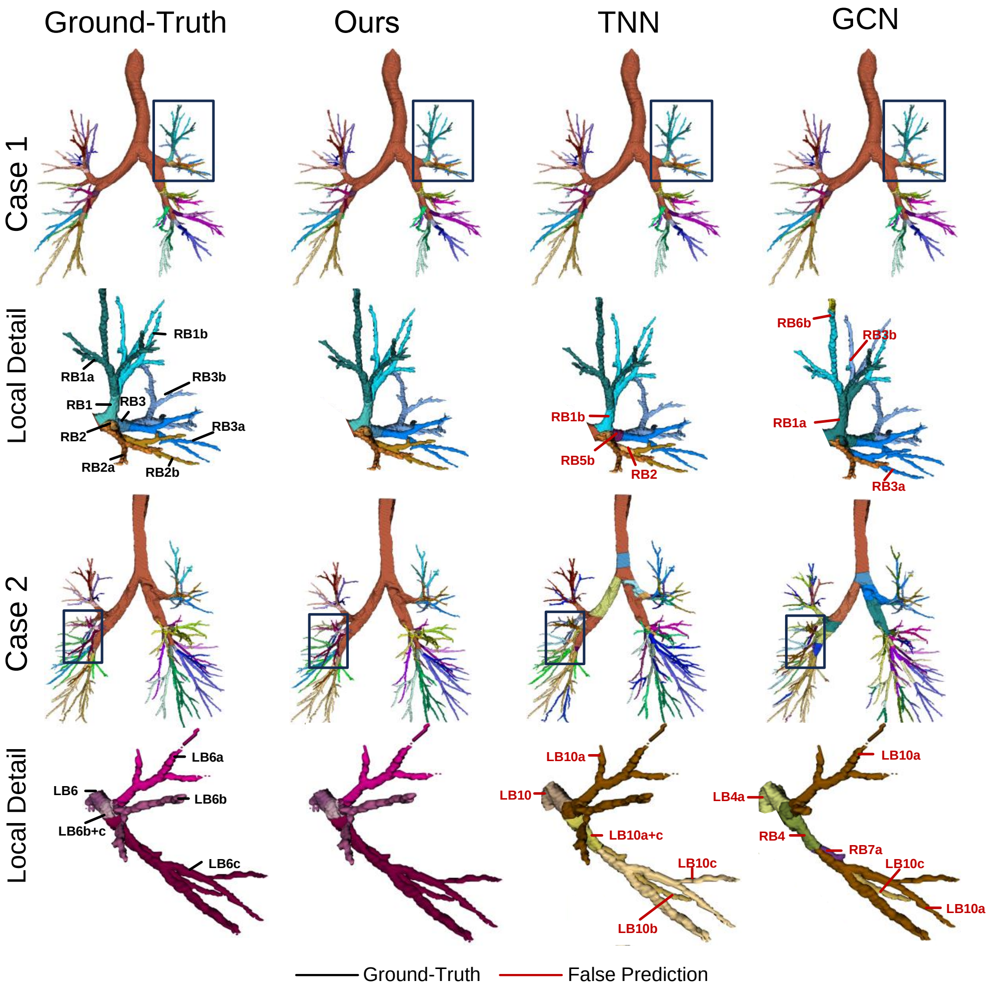

Fig. S5: Visualization of the quantitative comparison of the airway anatomical labeling. Case1 and Case2 are selected from ATM'22 and AIIB'23, respectively.

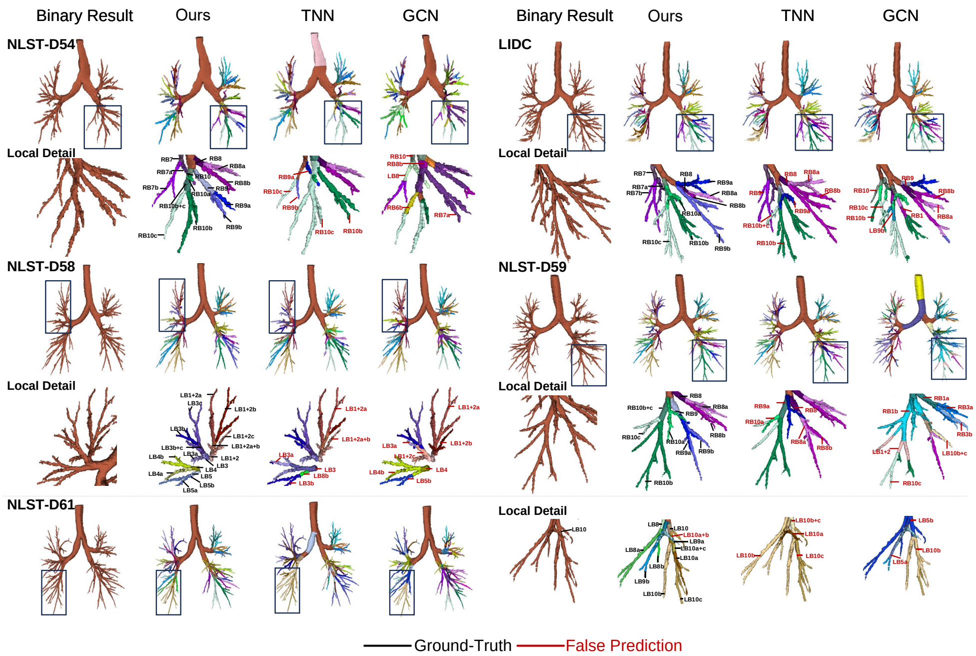

Fig. S6: Visualization of the qualitative comparison of the airway anatomical labeling.

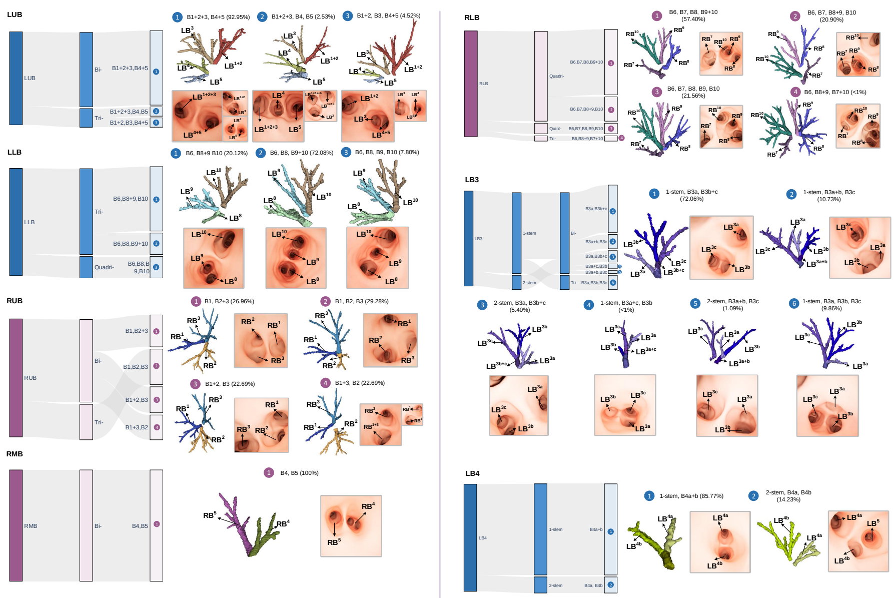

Fig. S7: Subfigure of the full branching patterns with endoscopic views (LUB, LLB, RUB, RLB, LB^3, LB^4).

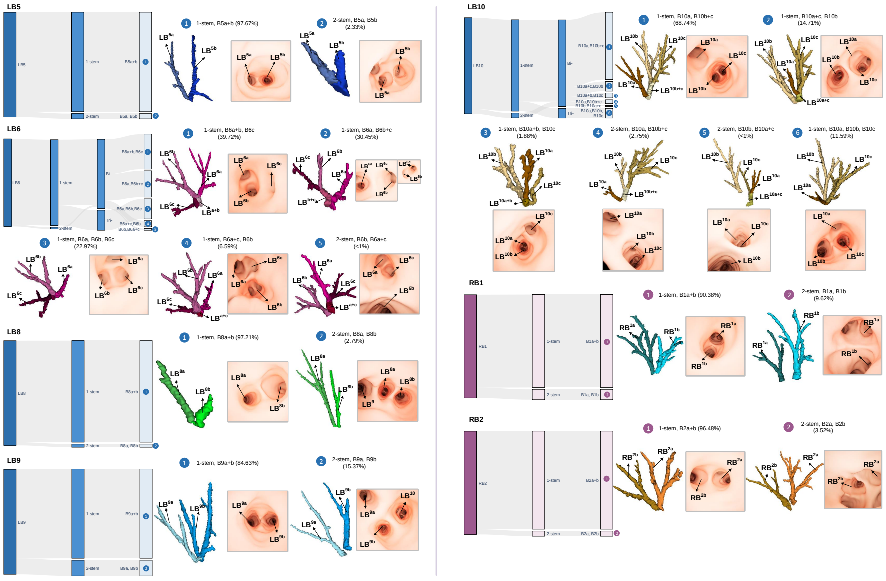

Fig. S8: Subfigure of the full branching patterns with endoscopic views (LB^5, LB^6, LB^8, LB^9, LB^{10}, RB^1, RB^2).

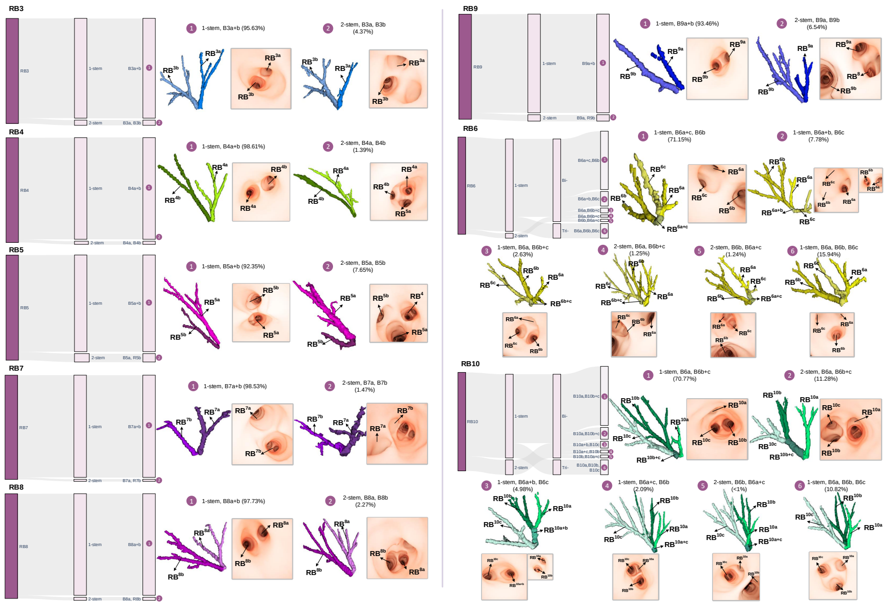

Fig. S9: Subfigure of the full branching patterns with endoscopic views (RB^3, RB^4, RB^5, RB^6, RB^7, RB^8, RB^9, RB^{10}).

Algorithm S1 Intra-Segment Pattern Analysis

Input:

`segment_labels`: Array of segment labels for each node

`generation`: Array of generation (depth) values for each node

`descendant_mask`: Binary matrix ($N \times N$), where `descendant_mask[i,j] = 1` if node i is an ancestor of node j

`lca_matrix`: Matrix ($N \times N$), where `lca_matrix[i,j]` is the lowest common ancestor (LCA) of nodes i and j

Output:

`Pattern_seg_intra`: A dictionary mapping each lobar block (from `LOBAR_SEGMENTS`) to clusters of segments based on the cotunk condition

`num_segment_classes` $\leftarrow 18$
for $i = 0$ to `num_segment_classes` -1 **do**
    Identify nodes in segment $i \rightarrow$ `segment_indices[`i`]`
    if `segment_indices[`i`]` is empty **then**
        Mark segment i as invalid
        continue
    end if
    Select representative node for segment i with minimum generation $\rightarrow$ `rep[`i`]`
end for
for each pair of segments (i, j) with $i \neq j$ **do**
    if either segment i or j is invalid **then**
        continue
    end if
    $lca_{ij} \leftarrow$ `lca_matrix[rep[`i`], rep[`j`]]`
    Extract descendant labels under lca_{ij} via `descendant_mask`
    if lca_{ij} = main bronchus **and** all descendant labels $\in \{i, j, \text{main bronchus}\}$ **then**
        Union segments i and j using union-find
    end if
end for
for each lobe in `LOBAR_SEGMENTS` (key = lobe, value = list of segment indices) **do**
    if any segment in the lobe is invalid **then**
        skip this lobe
    else
        Initialize union-find structure over segments within this lobe
        for each pair (i, j) in the lobe **do**
            if segments i and j satisfy the cotunk condition **then**
                Union i and j
            end if
        end for
        Extract clusters from the union-find structure
        `Pattern_seg_intra[lobe]` $\leftarrow$ clusters
    end if
end for
return `Pattern_seg_intra`

Algorithm S2 Intra-SubSegment Pattern Analysis

Input:

`segment_labels`: Array of segment labels for each node

`annotations`: Array of subsegment annotation values (0–6), where 0 represents root subsegment, 1–3 represent basic subsegments (a, b, c), and 4–6 represent co-tunk subsegments (a+b, b+c, a+c)

Output:

`Pattern_sub_intra`: Dictionary mapping each valid segment index (0–17) to a tuple `(stem_number, cotunk_type)`

Note: `cotunk_type` *will later be interpreted as monofurcation, bifurcation, or trifurcation*

```
num_segment_classes ← 18
Initialize RESULT as an array of shape (18 × 3): [valid flag, stem number, cotunk type]
for i = 0 to num_segment_classes −1 do
    Create a mask for nodes in segment i
    Determine existence flags for each subsegment (a, b, c, a+b, b+c, a+c)
    if segment i inherently allows only two basic subsegments (a and b) then
        if both a and b are detected then
            RESULT[i, valid] ← TRUE
            Set RESULT[i, stem_number] based on optional root presence
            RESULT[i, cotunk_type] ← 0                ▷ Interpret as monofurcation
        end if
    else
        if a, b, c are detected and at most one co-tunk subsegment is present then
            RESULT[i, valid] ← TRUE
            Determine cotunk_type based on detected co-tunk subsegment  ▷ e.g., a+b → bifurcation; none → trifurcation
            Set RESULT[i, stem_number] based on root presence and co-tunk configuration
        end if
    end if
end for
Initialize Pattern_sub_intra as empty dictionary
for each i such that RESULT[i, valid] is TRUE do
    Record (stem_number, cotunk_type) into Pattern_sub_intra[i]
end for
return Pattern_sub_intra
```

Algorithm S3 Inter-Subsegmental Pattern Analysis

Input:

`segment_labels`: Array of segment labels for each node
`subsegment_labels`: Array of subsegment labels for each node
`generation`: Array of generation values for each node
`descendant_mask`: Binary matrix ($N \times N$), where `descendant_mask[i,j] = 1` if node i is an ancestor of node j
`lca_matrix`: Matrix ($N \times N$), where `lca_matrix[i,j]` is the lowest common ancestor (LCA) of nodes i and j

Output:

`Pattern_sub_inter`: Dictionary mapping each inter-subsegment block to its clustered pattern result

```
Group nodes by subsegment label → indices_by_sub
Group nodes by segment label → indices_by_seg
Initialize SUB_COTUNK_INTER as a zero matrix
for each subsegment label i do
    if no nodes exist for i then
        continue
    end if
    Select representative node for i with minimum generation
    for j = 1 to i − 1 do
        if no nodes exist for j then
            continue
        end if
        if subsegments i and j belong to the same segment then
            Check predefined co-tunk rules
            if rule is satisfied then
                Mark connection between i and j in SUB_COTUNK_INTER
            end if
        end if
        Select representative node for subsegment j
        lca_ij ← lca_matrix[rep_i, rep_j]
        if lca_ij is main bronchus and all descendants ∈ {i, j, main bronchus} then
            Mark connection between i and j
        end if
    end for
    for each segment k do
        if i ∈ segment k then
            continue
        end if
        if nodes exist for segment k then
            Select representative node for segment k
            lca_ik ← lca_matrix[rep_i, rep_k]
            if all descendant nodes have segment_label = k or subsegment_label ∈ {i, main bronchus} then
                for each subsegment s in segment k do
                    Mark connection between i and s in SUB_COTUNK_INTER
                end for
            end if
        end if
    end for
end for
for each block in BLOCKS_INTER_SUB do
    if any corresponding segment is invalid based on intra-subsegment analysis then
        continue
    else
        Apply union-find clustering to subsegments in the block
        Apply uniform clustering to standardize the clusters
        Record result in Pattern_sub_inter[block]
    end if
end for
return Pattern_sub_inter
```

Algorithm S4 Computation of Stenosis ($\mathcal{S}$)

Require: Binary airway mask V_{airway}, spacing s, skeleton S, parsed skeleton S_{parse}, segment and lobe labels $Y_{\text{seg}}, Y_{\text{lob}}$

Ensure: Segmental and lobar stenosis scores

```
D ← EDT(V_airway, spacing = s)                         ▷ Euclidean distance transform
R ← D · S                                              ▷ Radius field along skeleton
L ← Unique labels from S_parse where l > 0
for all l ∈ L do
    r_min^(l) ← min(R[S_parse = l])
    r_mean^(l) ← mean(R[S_parse = l])
end for
for j = 0 to N_seg − 1 do
    if ∃l such that Y_seg[l] = j then
        Stenosis_seg[j] ← mean(1 − r_min^(l) / r_mean^(l))
    else
        Stenosis_seg[j] ← −1
    end if
end for
for k = 0 to N_lob − 1 do
    if ∃l such that Y_lob[l] = k + 1 then
        Stenosis_lob[k] ← mean(1 − r_min^(l) / r_mean^(l))
    else
        Stenosis_lob[k] ← −1
    end if
end for
return Stenosis_seg, Stenosis_lob
```

Algorithm S5 Computation of Ectasia ($\mathcal{E}$)

Require: Same inputs as Algorithm S4
Ensure: Segmental and lobar ectasia scores

for all $l \in L$ **do**
  $r_{\text{max}}^{(l)} \leftarrow \max(R[S_{\text{parse}} = l])$
  $r_{\text{mean}}^{(l)} \leftarrow \text{mean}(R[S_{\text{parse}} = l])$
end for
for $j = 0$ to $N_{\text{seg}} - 1$ **do**
  if $\exists l$ such that $Y_{\text{seg}}[l] = j$ **then**
    $\text{Ectasia}_{\text{seg}}[j] \leftarrow \text{mean}\left(\frac{r_{\text{max}}^{(l)}}{r_{\text{mean}}^{(l)}}\right)$
  else
    $\text{Ectasia}_{\text{seg}}[j] \leftarrow -1$
  end if
end for
for $k = 0$ to $N_{\text{lob}} - 1$ **do**
  if $\exists l$ such that $Y_{\text{lob}}[l] = k + 1$ **then**
    $\text{Ectasia}_{\text{lob}}[k] \leftarrow \text{mean}\left(\frac{r_{\text{max}}^{(l)}}{r_{\text{mean}}^{(l)}}\right)$
  else
    $\text{Ectasia}_{\text{lob}}[k] \leftarrow -1$
  end if
end for
return $\text{Ectasia}_{\text{seg}}$, $\text{Ectasia}_{\text{lob}}$

Algorithm S6 Computation of Tortuosity ($\mathcal{T}$)

Require: Voxel set Ω_l for a branch, voxel spacing s
Ensure: Tortuosity angle α

Convert Ω_l to physical space using s
Use PCA to find principal axis and endpoints S, E
Identify $P = \arg\max_{x_i \in \Omega_l} \text{dist}(x_i, \overline{SE})$
Compute $\alpha = \angle(\vec{PS}, \vec{PE})$
return α

Algorithm S7 Computation of Length ($\mathcal{L}$)

Require: Tree edge list, generation array, label array Y, nodewise lengths ℓ, target class K
Ensure: Mean geodesic length for class K

```
Identify all leaf nodes with label K
Compute their lowest common ancestor (LCA)
if LCA ∈ class K then
    Accumulate all Path(LCA → Leaf) lengths
else
    for all leaf nodes do
        Trace from LCA down to nearest node with label K
        Compute path length from this node to leaf
    end for
end if
return L_K
```

Algorithm S8 Computation of Divergence ($\mathcal{D}$)

Require: Tree edge list, generation array, label array Y, node coordinates $\mathbf{x}$, class label K
Ensure: Divergence angle θ in radians

```
Identify leaf nodes labeled as K
Compute their lowest common ancestor (LCA)
Let apex ← coordinate of LCA
for all leaf nodes i do
    v_i ← normalized vector from apex to leaf i
end for
Optimize unit vector u to maximize min_i⟨u, v_i⟩
Compute: θ = 2 · arccos(min_i⟨u, v_i⟩)
return θ
```

Algorithm S9 Computation of Complexity ($\mathcal{C}$)

Require: 3D skeleton volume S, class label mask Y, target class K
Ensure: Branch Complexity $\mathcal{C}$

```
Extract binary skeleton mask S_K = (S > 0) ∧ (Y = K)
Crop S_K to its minimal bounding box and pad to fixed size
for each box size s ∈ {2^1, ..., 2^k} do
    Count number N(s) of non-empty boxes of size s
end for
Perform linear regression on (log(1/s), log N(s))
return slope C
```

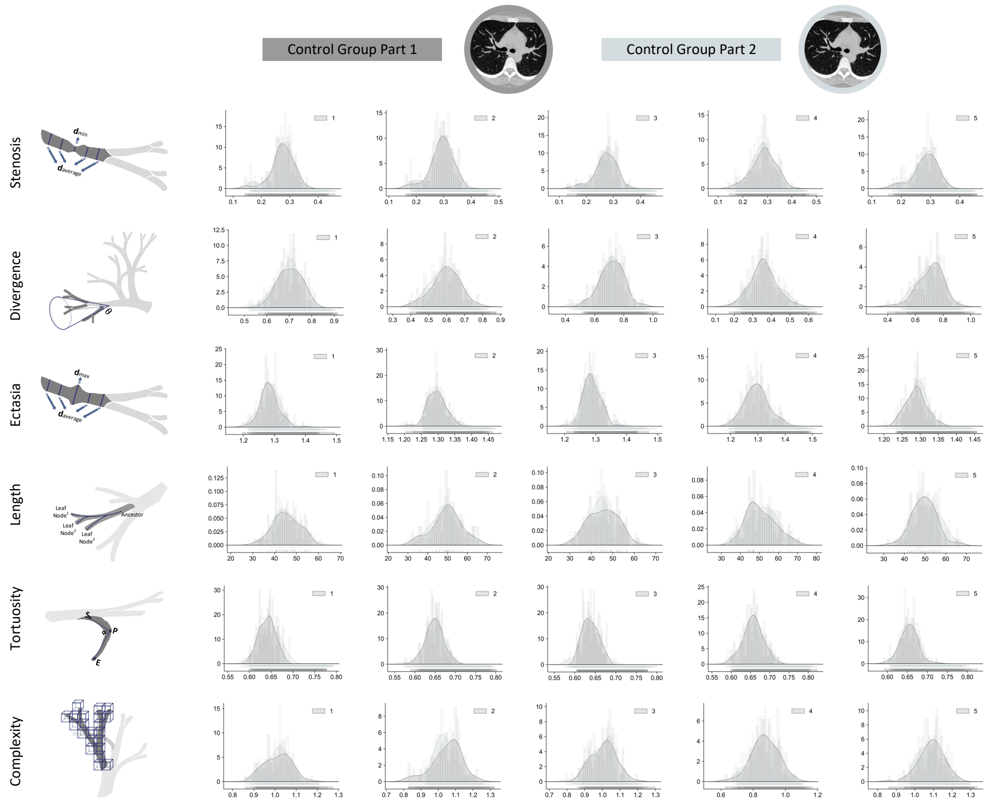

Fig. S10: Ablation study of the AirwaySignature within the healthy controls.

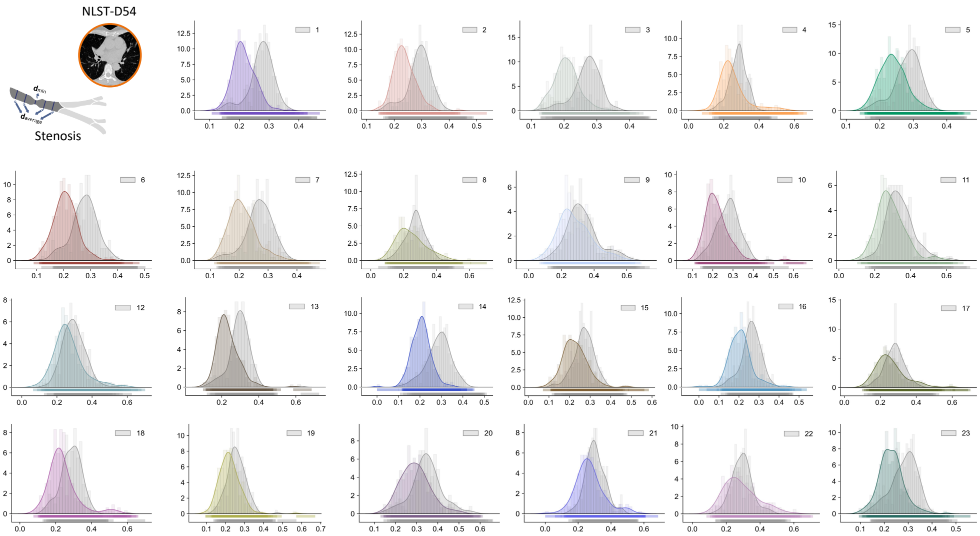

Fig. S11: Example of the Stenosis signature on all branches of the NLST-D54

Table S1: Quantative results on generalization performance with regard to the binary airway modeling on the cases with severe pulmonary fibrosis.

Airway Atlas: Binary Airway Modeling					
Lobar					
Method	**TLD**	**BND**	**DSC**	**clDice**	**Sensitivity**
UNet	46.43	49.36	62.39	58.76	54.89
nnUNet	48.06	49.97	61.97	59.67	54.65
AirMorph	**78.49**	**81.49**	**74.78**	**76.02**	**81.91**
Segmental					
Method	**TLD**	**BND**	**DSC**	**clDice**	**Sensitivity**
UNet	42.81	45.45	52.88	50.49	49.02
nnUNet	45.00	46.78	53.63	52.15	49.89
AirMorph	**73.48**	**76.80**	**68.30**	**69.69**	**75.99**
SubSegmental					
Method	**TLD**	**BND**	**DSC**	**clDice**	**Sensitivity**
UNet	40.23	43.73	42.43	43.7	41.13
nnUNet	43.03	46.29	44.15	46.41	42.56
AirMorph	**66.46**	**70.88**	**57.63**	**61.94**	**66.09**

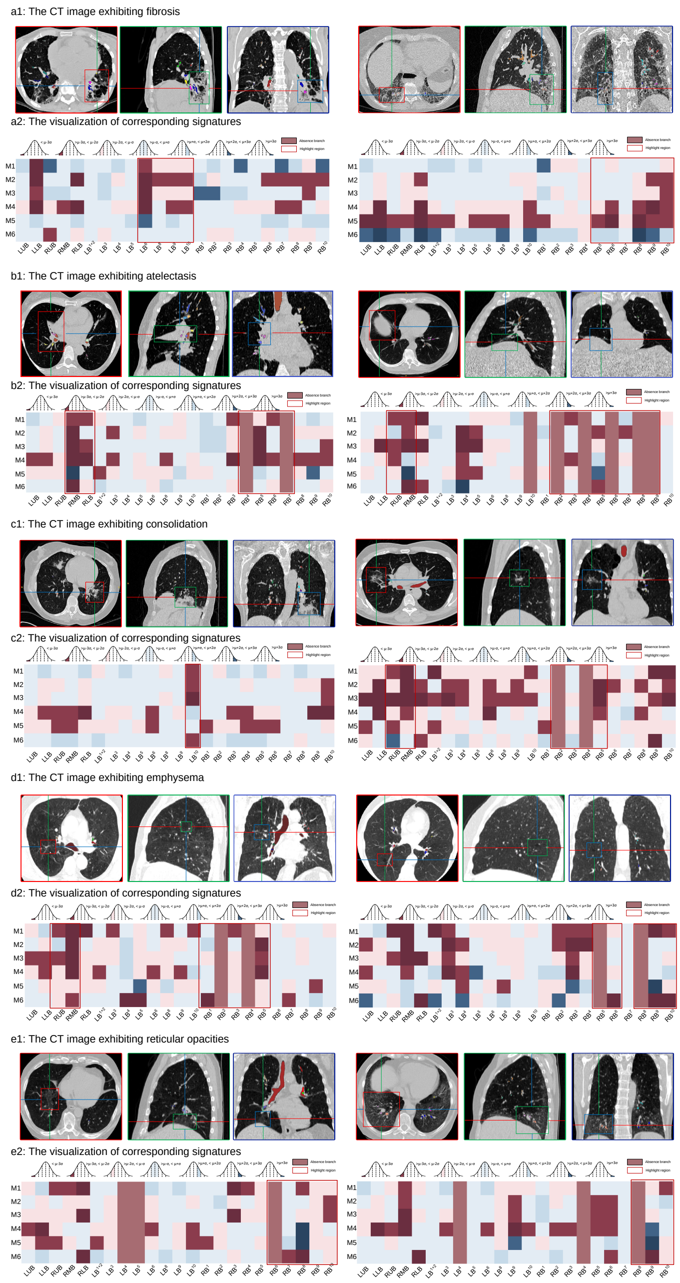

Fig. S12: AirwaySignature across all five lung diseases.

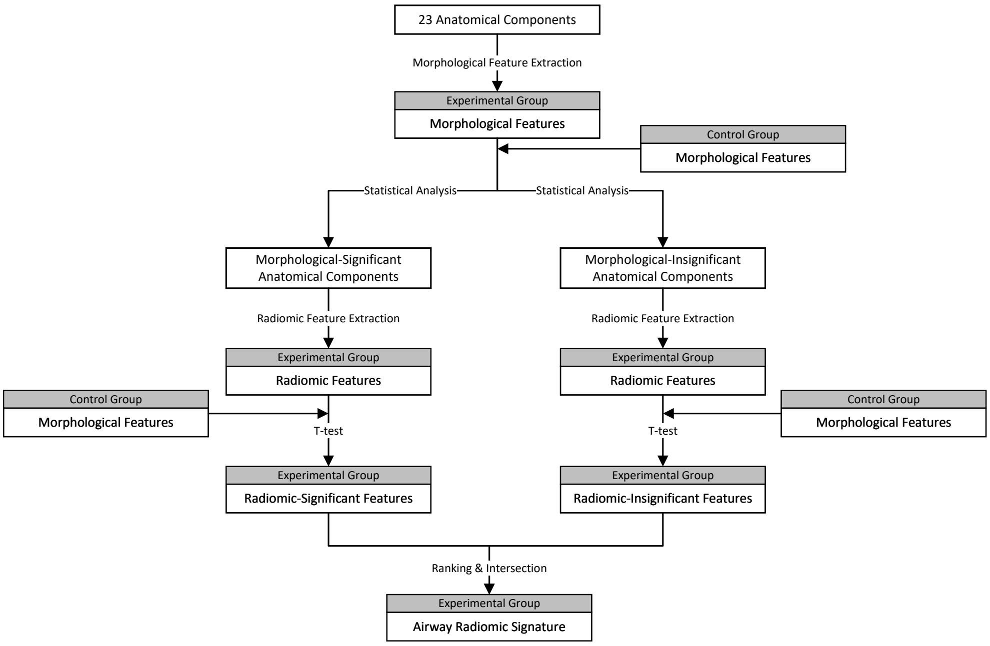

Fig. S13: Pipeline for Radiomic signature selection.

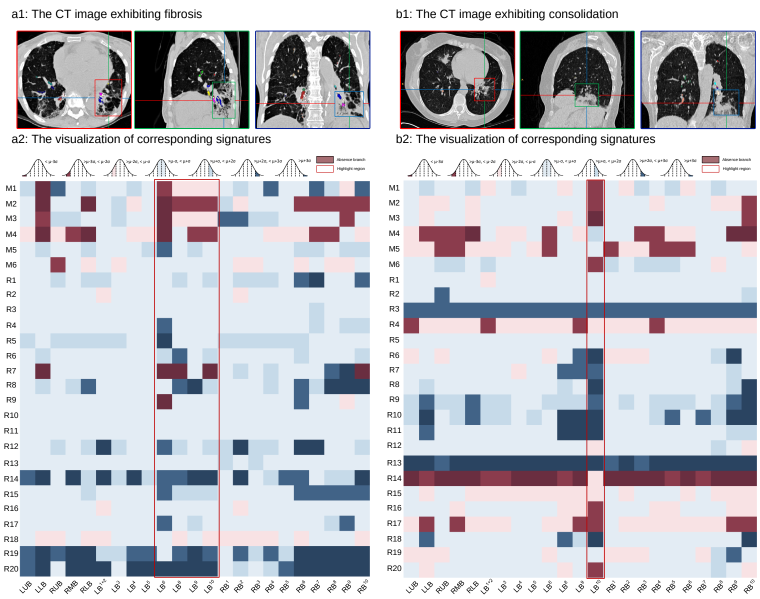

Fig. S14: Representative cases along with the radiomics features.

Table S2: Quantative results on generalization performance with regard to the anatomical airway labeling on the cases with severe pulmonary fibrosis.

Airway Atlas: Airway Anatomical Labeling					
Lobar					
Method	**TreeCons**	**TopoDist**	**Accuracy**	**Precision**	**Sensitivity**
GCN	91.60	0.6058	90.13	90.52	88.55
TNN	**99.35**	0.3069	95.18	93.93	94.04
AirMorph	98.73	**0.2382**	**97.20**	**97.04**	**96.23**
Segmental					
Method	**TreeCons**	**TopoDist**	**Accuracy**	**Precision**	**Sensitivity**
GCN	55.33	1.9646	66.93	60.25	65.69
TNN	81.34	1.1834	80.08	69.35	77.05
AirMorph	**97.26**	**0.6198**	**91.46**	**88.69**	**89.71**
SubSegmental					
Method	**TreeCons**	**TopoDist**	**Accuracy**	**Precision**	**Sensitivity**
GCN	51.49	3.8864	46.38	33.85	39.22
TNN	86.32	2.3539	65.61	53.39	59.48
AirMorph	**91.37**	**1.7423**	**83.52**	**80.59**	**81.62**

Table S3: Quantative results on graph building results.

Metrics	Skeletonization	SoftSkel-clDice	GBO-Skeleton	Ours
β_0 (Euler)	1.00 ± 0.00	1242.8 ± 407.5	1.00 ± 0.00	$\mathbf{1.00 \pm 0.00}$
β_1 (Euler)	16.55 ± 13.93	12.86 ± 7.23	16.55 ± 13.93	$\mathbf{0.00 \pm 0.00}$

Table S4: The comparative results of the binary airway modeling on the multi-site test cohorts.

Reconstructed Tree Length					
	LIDC-IDRI	NLST-D54	NLST-D58	NLST-D59	NLST-D61
UNet	1698.91 ± 842.67	1808.02 ± 636.40	1744.98 ± 597.87	2322.29 ± 817.41	2267.16 ± 790.48
nnUNet	1968.21 ± 939.96	1969.59 ± 628.83	1960.64 ± 613.45	2539.81 ± 873.58	2512.42 ± 803.66
AirMorph	$\mathbf{2876.13 \pm 1355.83}$	$\mathbf{3078.86 \pm 943.34}$	$\mathbf{2890.10 \pm 939.45}$	$\mathbf{3668.33 \pm 1294.32}$	$\mathbf{3643.27 \pm 1205.12}$
Reconstructed Branch Number					
	LIDC-IDRI	NLST-D54	NLST-D58	NLST-D59	NLST-D61
UNet	88.61 ± 52.70	92.93 ± 36.47	87.82 ± 34.98	134.43 ± 55.66	137.23 ± 56.40
nnUNet	97.98 ± 54.83	97.47 ± 34.75	95.28 ± 34.12	131.90 ± 48.86	133.04 ± 46.12
AirMorph	$\mathbf{157.92 \pm 84.45}$	$\mathbf{170.93 \pm 54.34}$	$\mathbf{154.83 \pm 52.48}$	$\mathbf{205.42 \pm 78.45}$	$\mathbf{209.21 \pm 74.86}$

Table S5: The comparative results of the airway anatomical labeling on the multi-site test cohorts.

TreeCons					
	LIDC-IDRI	NLST-D54	NLST-D58	NLST-D59	NLST-D61
GCN	36.86 ± 11.07	40.63 ± 7.89	39.22 ± 8.55	44.13 ± 8.38	44.56 ± 8.03
TNN	58.74 ± 12.52	62.63 ± 8.14	60.16 ± 8.47	66.00 ± 8.92	66.58 ± 8.15
AirMorph	**89.57 ± 12.52**	**93.90 ± 4.89**	**93.72 ± 5.07**	**95.36 ± 3.54**	**95.28 ± 4.22**
TopoDist					
	LIDC-IDRI	NLST-D54	NLST-D58	NLST-D59	NLST-D61
GCN	1.95 ± 0.37	1.92 ± 0.28	1.86 ± 0.24	1.94 ± 0.28	1.96 ± 0.31
nnUNet	1.42 ± 0.24	1.40 ± 0.17	1.40 ± 0.16	1.35 ± 0.17	1.35 ± 0.18
AirMorph	**1.17 ± 0.27**	**1.11 ± 0.07**	**1.11 ± 0.08**	**1.10 ± 0.07**	**1.11 ± 0.11**

Table S6: Ablation study of the graph building on ATM'22 internal testset.

Lobar						
Method	**GraphBuild**	**TreeCons**	**TopoDist**	**Accuracy**	**Precision**	**Sensitivity**
GCN	Skeletonization	95.71	0.29717	94.11	94.25	91.23
	MPC-Skel (Ours)	98.16	0.12249	96.73	96.64	95.77
	Ablation: HRLP	87.24	2.11652	74.60	78.70	70.23
	Ablation: LRHP	98.88	0.0971	96.41	96.48	95.51
TNN	Skeletonization	97.75	0.62867	91.95	91.82	90.61
	MPC-Skel (Ours)	100.00	0.03492	98.00	98.02	96.82
	Ablation: HRLP	94.79	2.25155	76.59	73.50	73.13
	Ablation: LRHP	98.72	0.48659	91.29	89.54	90.16
AirMorph	Skeletonization	98.45	0.09023	97.72	97.92	96.29
	MPC-Skel (Ours)	99.99	0.02603	99.06	99.20	98.52
	Ablation: HRLP	89.26	1.48449	81.57	82.19	79.39
	Ablation: LRHP	99.87	0.03092	98.65	98.81	98.31
Segmental						
Method	**GraphBuild**	**TreeCons**	**TopoDist**	**Accuracy**	**Precision**	**Sensitivity**
GCN	Skeletonization	63.93	1.63591	75.29	68.91	74.31
	MPC-Skel (Ours)	67.38	0.90323	83.09	75.92	81.51
	Ablation: HRLP	49.40	4.79132	46.80	42.73	49.21
	Ablation: LRHP	63.45	0.87471	82.15	73.58	80.85
TNN	Skeletonization	83.56	1.34551	80.56	70.94	78.18
	MPC-Skel (Ours)	83.46	0.41358	89.16	79.59	87.18
	Ablation: HRLP	76.86	4.46636	53.86	43.88	52.72
	Ablation: LRHP	71.56	1.70571	71.67	58.54	67.41
AirMorph	Skeletonization	96.40	0.46364	92.71	91.92	92.88
	MPC-Skel (Ours)	99.47	0.10241	97.42	96.84	97.12
	Ablation: HRLP	82.16	4.55093	60.15	55.81	60.44
	Ablation: LRHP	99.08	0.14258	96.48	94.77	95.41
SubSegmental						
Method	**GraphBuild**	**TreeCons**	**TopoDist**	**Accuracy**	**Precision**	**Sensitivity**
GCN	Skeletonization	57.73	3.27129	55.85	45.94	49.05
	MPC-Skel (Ours)	65.93	2.27723	63.89	52.83	57.31
	Ablation: HRLP	35.12	7.25278	25.52	14.69	17.67
	Ablation: LRHP	67.93	3.15233	62.88	51.53	56.25
TNN	Skeletonization	79.54	4.14947	52.20	39.50	45.46
	MPC-Skel (Ours)	86.32	2.35388	65.61	53.39	59.48
	Ablation: HRLP	69.46	7.01118	36.15	23.69	28.67
	Ablation: LRHP	81.86	3.90828	57.38	43.84	48.62
AirMorph	Skeletonization	90.76	1.06177	87.65	85.71	86.40
	MPC-Skel (Ours)	98.02	0.48075	94.12	93.12	93.33
	Ablation: HRLP	62.04	4.71749	53.18	43.34	45.88
	Ablation: LRHP	97.44	1.73777	90.69	89.82	89.76

Table S7: Ablation study of the graph building on AIIB'23 internal testset.

Lobar						
Method	**GraphBuild**	**TreeCons**	**TopoDist**	**Accuracy**	**Precision**	**Sensitivity**
GCN	Skeletonization	90.43	1.1117	85.49	86.82	81.82
	MPC-Skel (Ours)	91.60	0.60576	90.13	90.52	88.55
	Ablation: HRLP	87.45	2.16909	76.57	78.59	71.37
	Ablation: LRHP	89.51	0.75638	87.41	87.84	87.02
TNN	Skeletonization	96.41	1.06921	86.56	84.99	84.90
	MPC-Skel (Ours)	99.35	0.30692	95.18	93.93	94.04
	Ablation: HRLP	94.79	2.25155	76.59	73.50	73.13
	Ablation: LRHP	98.72	0.48659	91.29	89.54	90.16
AirMorph	Skeletonization	95.71	0.53392	93.96	94.06	92.18
	MPC-Skel (Ours)	98.73	0.23820	97.20	97.04	96.23
	Ablation: HRLP	89.13	1.37233	84.26	84.82	82.45
	Ablation: LRHP	97.17	0.29594	95.62	95.36	94.99
Segmental						
Method	**GraphBuild**	**TreeCons**	**TopoDist**	**Accuracy**	**Precision**	**Sensitivity**
GCN	Skeletonization	55.75	3.10851	59.43	54.45	58.90
	MPC-Skel (Ours)	55.33	1.96458	66.93	60.25	65.69
	Ablation: HRLP	49.62	5.35382	44.81	40.76	46.58
	Ablation: LRHP	49.35	2.15344	65.08	55.61	64.40
TNN	Skeletonization	81.04	2.60559	66.46	56.10	63.51
	MPC-Skel (Ours)	81.34	1.18344	80.08	69.35	77.05
	Ablation: HRLP	76.86	4.46636	53.86	43.88	52.72
	Ablation: LRHP	71.56	1.70571	71.67	58.54	67.41
AirMorph	Skeletonization	90.52	1.61192	84.50	81.87	83.21
	MPC-Skel (Ours)	97.26	0.61977	91.46	88.69	89.71
	Ablation: HRLP	78.29	4.48236	61.79	58.44	62.38
	Ablation: LRHP	96.71	0.90482	87.45	81.36	83.75
SubSegmental						
Method	**GraphBuild**	**TreeCons**	**TopoDist**	**Accuracy**	**Precision**	**Sensitivity**
GCN	Skeletonization	44.09	5.20294	39.24	27.44	30.78
	MPC-Skel (Ours)	51.49	3.88637	46.38	33.85	39.22
	Ablation: HRLP	35.62	7.80358	25.69	15.69	18.27
	Ablation: LRHP	53.49	5.17098	44.27	30.43	36.20
TNN	Skeletonization	69.46	7.01118	36.15	23.69	28.67
	MPC-Skel (Ours)	79.54	4.14947	52.20	39.50	45.46
	Ablation: HRLP	69.46	7.01118	36.15	23.69	28.67
	Ablation: LRHP	81.86	3.90828	57.38	43.84	48.62
AirMorph	Skeletonization	78.38	2.75415	75.57	71.48	72.81
	MPC-Skel (Ours)	91.37	1.74228	83.52	80.59	81.62
	Ablation: HRLP	57.39	5.35355	53.86	46.56	48.53
	Ablation: LRHP	89.28	4.00417	77.41	72.95	73.22

Table S8: Statistical analysis of diverse airway branching patterns of ATM'22 dataset.

		Mono-	Bi-	Tri-	Quadri-
LUB B1-5			B1+2+3,B4+5 (96.94%)	B1+2+3,B4,B5 (1.02%)	
				B1+2,B3,B4+5 (2.04%)	
LLB B6-10				B6,B8+9,B10 (39.18%)	B6,B8,B9,B10 (7.22%)
				B6,B8,B9+10 (53.61%)	
LB1+2	1-stem		B1+2a+b,B1+2c (72.45%)	B1+2a,B1+2b,B1+2c (<1%)	
			B1+2a,B1+2b+c (12.45%)		
			B1+2a+c,B1+2b (<1%)		
	2-stem		B1+2a+b,B1+2c (19.90%)		
			B1+2a,B1+2b+c (<1%)		
LB3	1-stem		B3a+b,B3c (12.76%)	B3a,B3b,B3c (9.86%)	
			B3a,B3b+c (68.88%)		
			B3a+c,B3b (<1%)		
	2-stem		B3a+b,B3c (<1%)		
			B3a,B3b+c (6.12%)		
LB4	1-stem	B4a+b (78.76%)			
	2-stem		B4a,B4b (21.24%)		
LB5	1-stem	B5a+b (100%)			
	2-stem		B5a,B5b (<1%)		
LB6	1-stem		B6a+b,B6c (42.02%)	B6a,B6b,B6c (15.96%)	
			B6a,B6b+c (35.11%)		
			B6a+c,B6b (5.85%)		
	2-stem		B6b,B6a+c (1.06%)		
LB8	1-stem	B8a+b (97.91%)			
	2-stem		B8a,B8b (2.09%)		
LB9	1-stem	B9a+b (93.12%)			
	2-stem		B9a,B9b (2.88%)		
LB10	1-stem		B10a+b,B10c (2.65%)	B10a,B10b,B10c (6.35%)	
			B10a,B10b+c (72.49%)		
			B10a+c,B10b (17.46%)		
	2-stem		B10a,B10b+c (<1%)		
			B10b,B10a+c (<1%)		

		Mono-	Bi-	Tri-	Quadri-	Quint-
RUB B1-3			B1+2,B3 (31.63%)	B1,B2,B3 (21.94%)		
			B1+3,B2 (19.90%)			
			B1,B2+3 (26.53%)			
RMB B4-5			B4,B5 (100%)			
RLB B6-10				B6,B8+9,B7+10 (1.14%)	B6,B7,B8+9,B10 (39.20%)	B6,B7,B8,B9,B10 (9.09%)
					B6,B7,B8,B9+10 (50.57%)	
RB1	1-stem	B1a+b (82.14%)				
	2-stem		B1a,B1b (17.86%)			
RB2	1-stem	B2a+b (97.96%)				
	2-stem		B2a,B2b (2.04%)			
RB3	1-stem	B3a+b (95.90%)				
	2-stem		B3a,B3b (4.10%)			
RB4	1-stem	B4a+b (100%)				
	2-stem		B4a,B4b (<1%)			
RB5	1-stem	B5a+b (94.36%)				
	2-stem		B5a,B5b (5.64%)			
RB6	1-stem		B6a+b,B6c (10.88%)	B6a,B6b,B6c (28.50%)		
			B6a,B6b+c (4.15%)			
			B6a+c,B6b (55.96%)			
	2-stem		B6a,B6b+c (<1%)			
			B6b,B6a+c (<1%)			
RB7	1-stem	B7a+b (100%)				
	2-stem		B7a,B7b (<1%)			
RB8	1-stem	B8a+b (99.49%)				
	2-stem		B8a,B8b (<1%)			
RB9	1-stem	B9a+b (93.78%)				
	2-stem		B9a+b (6.22%)			
RB10	1-stem		B10a+b,B10c (7.69%)	B10a,B10b,B10c (4.62%)		
			B10a,B10b+c (76.92%)			
			B10a+c,B10b (4.62%)			
	2-stem		B10a,B10b+c (5.64%)			
			B10b,B10a+c (<1%)			

Table S9: Statistical analysis of diverse airway branching patterns of AIIB'23 dataset.

		Mono-	Bi-	Tri-	Quadri-
LUB B1-5			B1+2+3,B4+5 (90.24%)	B1+2+3,B4,B5 (2.44%)	
				B1+2,B3,B4+5 (7.32%)	
LLB B6-10				B6,B8+9,B10 (21.18%)	B6,B8,B9,B10 (4.71%)
				B6,B8,B9+10 (74.12%)	
LB1+2	1-stem		B1+2a+b,B1+2c (65.00%)	B1+2a,B1+2b,B1+2c (3.75%)	
			B1+2a,B1+2b+c (17.50%)		
			B1+2a+c,B1+2b (3.75%)		
	2-stem		B1+2a+b,B1+2c (7.50%)		
			B1+2a,B1+2b+c (2.50%)		
LB3	1-stem		B3a+b,B3c (15.66%)	B3a,B3b,B3c (7.23%)	
			B3a,B3b+c (61.45%)		
			B3a+c,B3b (4.82%)		
	2-stem		B3a+b,B3c (2.41%)		
			B3a,B3b+c (8.43%)		
LB4	1-stem	B4a+b (90.54%)			
	2-stem		B4a,B4b (9.46%)		
LB5	1-stem	B5a+b (96.83%)			
	2-stem		B5a,B5b (3.17%)		
LB6	1-stem		B6a+b,B6c (48.72%)	B6a,B6b,B6c (16.67%)	
			B6a,B6b+c (30.77%)		
			B6a+c,B6b (3.85%)		
	2-stem		B6b,B6a+c (<1%)		
LB8	1-stem	B8a+b (98.80%)			
	2-stem		B8a,B8b (1.20%)		
LB9	1-stem	B9a+b (86.08%)			
	2-stem		B9a,B9b (13.92%)		
LB10	1-stem		B10a+b,B10c (1.27%)	B10a,B10b,B10c (6.33%)	
			B10a,B10b+c (70.89%)		
			B10a+c,B10b (18.99%)		
	2-stem		B10a,B10b+c (2.53%)		
			B10b,B10a+c (<1%)		

		Mono-	Bi-	Tri-	Quadri-	Quint-
RUB B1-3			B1+2,B3 (20.00%)	B1,B2,B3 (30.59%)		
			B1+3,B2 (20.00%)			
			B1,B2+3 (29.41%)			
RMB B4-5			B4,B5 (100%)			
RLB B6-10				B6,B8+9,B7+10 (<1%)	B6,B7,B8+9,B10 (25.64%)	B6,B7,B8,B9,B10 (14.10%)
					B6,B7,B8,B9+10 (60.26%)	
RB1	1-stem	B1a+b (94.12%)				
	2-stem		B1a,B1b (5.88%)			
RB2	1-stem	B2a+b (96.47%)				
	2-stem		B2a,B2b (3.53%)			
RB3	1-stem	B3a+b (98.82%)				
	2-stem		B3a,B3b (1.18%)			
RB4	1-stem	B4a+b (98.78%)				
	2-stem		B4a,B4b (1.22%)			
RB5	1-stem	B5a+b (95.12%)				
	2-stem		B5a,B5b (4.88%)			
RB6	1-stem		B6a+b,B6c (14.10%)	B6a,B6b,B6c (14.10%)		
			B6a,B6b+c (3.85%)			
			B6a+c,B6b (62.82%)			
	2-stem		B6a,B6b+c (3.85%)			
			B6b,B6a+c (1.28%)			
RB7	1-stem	B7a+b (98.65%)				
	2-stem		B7a,B7b (1.35%)			
RB8	1-stem	B8a+b (100%)				
	2-stem		B8a,B8b (<1%)			
RB9	1-stem	B9a+b (90.91%)				
	2-stem		B9a+b (9.09%)			
RB10	1-stem		B10a+b,B10c (9.09%)	B10a,B10b,B10c (7.79%)		
			B10a,B10b+c (72.73%)			
			B10a+c,B10b (1.30%)			
	2-stem		B10a,B10b+c (9.09%)			
			B10b,B10a+c (<1%)			

Table S10: Statistical analysis of diverse airway branching patterns of LIDC-IDRI dataset.

		Mono-	Bi-	Tri-	Quadri-
LUB B1-5			B1+2+3,B4+5 (93.68%)	B1+2+3,B4,B5 (3.05%)	
				B1+2,B3,B4+5 (3.27%)	
LLB B6-10				B6,B8+9,B10 (14.67%)	B6,B8,B9,B10 (8.60%)
				B6,B8,B9+10 (76.73%)	
LB1+2	1-stem		B1+2a+b,B1+2c (67.89%)	B1+2a,B1+2b,B1+2c (8.27%)	
			B1+2a,B1+2b+c (9.70%)		
			B1+2a+c,B1+2b (<1%)		
	2-stem		B1+2a+b,B1+2c (12.72%)		
			B1+2a,B1+2b+c (1.27%)		
LB3	1-stem		B3a+b,B3c (9.44%)	B3a,B3b,B3c (12.70%)	
			B3a,B3b+c (71.69%)		
			B3a+c,B3b (1.09%)		
	2-stem		B3a+b,B3c (<1%)		
			B3a,B3b+c (4.17%)		
LB4	1-stem	B4a+b (84.91%)			
	2-stem		B4a,B4b (15.09%)		
LB5	1-stem	B5a+b (95.38%)			
	2-stem		B5a,B5b (4.62%)		
LB6	1-stem		B6a+b,B6c (31.45%)	B6a,B6b,B6c (29.86%)	
			B6a,B6b+c (31.45%)		
			B6a+c,B6b (6.54%)		
	2-stem		B6b,B6a+c (<1%)		
LB8	1-stem	B8a+b (93.12%)			
	2-stem		B8a,B8b (6.88%)		
LB9	1-stem	B9a+b (80.26%)			
	2-stem		B9a,B9b (19.74%)		
LB10	1-stem		B10a+b,B10c (1.60%)	B10a,B10b,B10c (15.17%)	
			B10a,B10b+c (66.67%)		
			B10a+c,B10b (11.38%)		
	2-stem		B10a,B10b+c (4.99%)		
			B10b,B10a+c (<1%)		

		Mono-	Bi-	Tri-	Quadri-	Quint-
RUB B1-3			B1+2,B3 (26.55%)	B1,B2,B3 (30.17%)		
			B1+3,B2 (19.48%)			
			B1,B2+3 (23.79%)			
RMB B4-5			B4,B5 (100%)			
RLB B6-10				B6,B8+9,B7+10 (<1%)	B6,B7,B8+9,B10 (17.29%)	B6,B7,B8,B9,B10 (16.85%)
					B6,B7,B8,B9+10 (65.85%)	
RB1	1-stem	B1a+b (86.27%)				
	2-stem		B1a,B1b (13.73%)			
RB2	1-stem	B2a+b (92.72%)				
	2-stem		B2a,B2b (7.28%)			
RB3	1-stem	B3a+b (94.40%)				
	2-stem		B3a,B3b (5.60%)			
RB4	1-stem	B4a+b (97.28%)				
	2-stem		B4a,B4b (2.72%)			
RB5	1-stem	B5a+b (88.30%)				
	2-stem		B5a,B5b (11.70%)			
RB6	1-stem		B6a+b,B6c (6.81%)	B6a,B6b,B6c (19.07%)		
			B6a,B6b+c (1.95%)			
			B6a+c,B6b (68.09%)			
	2-stem		B6a,B6b+c (2.53%)			
			B6b,B6a+c (1.56%)			
RB7	1-stem	B7a+b (95.24%)				
	2-stem		B7a,B7b (4.76%)			
RB8	1-stem	B8a+b (91.84%)				
	2-stem		B8a,B8b (8.16%)			
RB9	1-stem	B9a+b (91.42%)				
	2-stem		B9a+b (8.58%)			
RB10	1-stem		B10a+b,B10c (5.57%)	B10a,B10b,B10c (13.05%)		
			B10a,B10b+c (65.64%)			
			B10a+c,B10b (1.34%)			
	2-stem		B10a,B10b+c (14.40%)			
			B10b,B10a+c (<1%)			

Table S11: Statistical analysis of diverse airway branching patterns of NLST-D54 dataset.

		Mono-	Bi-	Tri-	Quadri-
LUB B1-5			B1+2+3,B4+5 (94.58%)	B1+2+3,B4,B5 (2.46%)	
				B1+2,B3,B4+5 (2.96%)	
LLB B6-10				B6,B8+9,B10 (13.36%)	B6,B8,B9,B10 (8.29%)
				B6,B8,B9+10 (78.34%)	
LB1+2	1-stem		B1+2a+b,B1+2c (66.52%)	B1+2a,B1+2b,B1+2c (7.69%)	
			B1+2a,B1+2b+c (14.48%)		
			B1+2a+c,B1+2b (<1%)		
	2-stem		B1+2a+b,B1+2c (10.41%)		
			B1+2a,B1+2b+c (<1%)		
LB3	1-stem		B3a+b,B3c (8.21%)	B3a,B3b,B3c (7.18%)	
			B3a,B3b+c (79.49%)		
			B3a+c,B3b (<1%)		
	2-stem		B3a+b,B3c (<1%)		
			B3a,B3b+c (4.62%)		
LB4	1-stem	B4a+b (83.33%)			
	2-stem		B4a,B4b (16.67%)		
LB5	1-stem	B5a+b (95.86%)			
	2-stem		B5a,B5b (4.14%)		
LB6	1-stem		B6a+b,B6c (34.40%)	B6a,B6b,B6c (29.82%)	
			B6a,B6b+c (28.44%)		
			B6a+c,B6b (7.34%)		
	2-stem		B6b,B6a+c (<1%)		
LB8	1-stem	B8a+b (98.68%)			
	2-stem		B8a,B8b (1.32%)		
LB9	1-stem	B9a+b (80.88%)			
	2-stem		B9a,B9b (19.12%)		
LB10	1-stem		B10a+b,B10c (3.49%)	B10a,B10b,B10c (15.70%)	
			B10a,B10b+c (66.86%)		
			B10a+c,B10b (9.88%)		
	2-stem		B10a,B10b+c (2.91%)		
			B10b,B10a+c (1.16%)		

		Mono-	Bi-	Tri-	Quadri-	Quint-
RUB B1-3			B1+2,B3 (15.72%)	B1,B2,B3 (31.00%)		
			B1+3,B2 (27.07%)			
			B1,B2+3 (26.20%)			
RMB B4-5			B4,B5 (100%)			
RLB B6-10				B6,B8+9,B7+10 (<1%)	B6,B7,B8+9,B10 (15.61%)	B6,B7,B8,B9,B10 (28.90%)
					B6,B7,B8,B9+10 (55.49%)	
RB1	1-stem	B1a+b (91.60%)				
	2-stem		B1a,B1b (8.40%)			
RB2	1-stem	B2a+b (96.96%)				
	2-stem		B2a,B2b (3.04%)			
RB3	1-stem	B3a+b (95.67%)				
	2-stem		B3a,B3b (4.33%)			
RB4	1-stem	B4a+b (97.75%)				
	2-stem		B4a,B4b (2.25%)			
RB5	1-stem	B5a+b (92.67%)				
	2-stem		B5a,B5b (7.33%)			
RB6	1-stem		B6a+b,B6c (5.29%)	B6a,B6b,B6c (15.87%)		
			B6a,B6b+c (1.92%)			
			B6a+c,B6b (74.52%)			
	2-stem		B6a,B6b+c (<1%)			
			B6b,B6a+c (1.44%)			
RB7	1-stem	B7a+b (98.58%)				
	2-stem		B7a,B7b (1.42%)			
RB8	1-stem	B8a+b (96.53%)				
	2-stem		B8a,B8b (3.47%)			
RB9	1-stem	B9a+b (95.39%)				
	2-stem		B9a+b (4.61%)			
RB10	1-stem		B10a+b,B10c (2.66%)	B10a,B10b,B10c (16.49%)		
			B10a,B10b+c (60.11%)			
			B10a+c,B10b (3.19%)			
	2-stem		B10a,B10b+c (17.55%)			
			B10b,B10a+c (<1%)			

Table S12: Statistical analysis of diverse airway branching patterns of NLST-D58 dataset.

		Mono-	Bi-	Tri-	Quadri-
LUB B1-5			B1+2+3,B4+5 (93.33%)	B1+2+3,B4,B5 (2.96%) B1+2,B3,B4+5 (3.70%)	
LLB B6-10				B6,B8+9,B10 (23.84%) B6,B8,B9+10 (68.87%)	B6,B8,B9,B10 (7.28%)
LB1+2	1-stem		B1+2a+b,B1+2c (76.82%) B1+2a,B1+2b+c (7.95%) B1+2a+c,B1+2b (<1%)	B1+2a,B1+2b,B1+2c (6.62%)	
	2-stem		B1+2a+b,B1+2c (8.61%) B1+2a,B1+2b+c (<1%)		
LB3	1-stem		B3a+b,B3c (12.21%) B3a,B3b+c (72.52%) B3a+c,B3b (<1%)	B3a,B3b,B3c (10.69%)	
	2-stem		B3a+b,B3c (<1%) B3a,B3b+c (3.82%)		
LB4	1-stem	B4a+b (89.47%)			
	2-stem		B4a,B4b (10.53%)		
LB5	1-stem	B5a+b (98.29%)			
	2-stem		B5a,B5b (1.71%)		
LB6	1-stem		B6a+b,B6c (42.11%) B6a,B6b+c (29.32%) B6a+c,B6b (6.02%)	B6a,B6b,B6c (22.56%)	
	2-stem		B6b,B6a+c (<1%)		
LB8	1-stem	B8a+b (96.49%)			
	2-stem		B8a,B8b (3.51%)		
LB9	1-stem	B9a+b (85.61%)			
	2-stem		B9a,B9b (14.39%)		
LB10	1-stem		B10a+b,B10c (2.36%) B10a,B10b+c (59.84%) B10a+c,B10b (16.54%)	B10a,B10b,B10c (18.11%)	
	2-stem		B10a,B10b+c (3.15%) B10b,B10a+c (<1%)		

		Mono-	Bi-	Tri-	Quadri-	Quint-
RUB B1-3			B1+2,B3 (19.05%) B1+3,B2 (21.77%) B1,B2+3 (23.81%)	B1,B2,B3 (35.37%)		
RMB B4-5			B4,B5 (100%)			
RLB B6-10				B6,B8+9,B7+10 (<1%)	B6,B7,B8+9,B10 (12.61%) B6,B7,B8,B9+10 (54.95%)	B6,B7,B8,B9,B10 (32.43%)
RB1	1-stem	B1a+b (96.51%)				
	2-stem		B1a,B1b (3.49%)			
RB2	1-stem	B2a+b (96.03%)				
	2-stem		B2a,B2b (3.97%)			
RB3	1-stem	B3a+b (95.36%)				
	2-stem		B3a,B3b (4.64%)			
RB4	1-stem	B4a+b (98.18%)				
	2-stem		B4a,B4b (1.82%)			
RB5	1-stem	B5a+b (87.07%)				
	2-stem		B5a,B5b (12.93%)			
RB6	1-stem		B6a+b,B6c (5.84%) B6a,B6b+c (1.46%) B6a+c,B6b (76.64%)	B6a,B6b,B6c (13.87%)		
	2-stem		B6a,B6b+c (<1%) B6b,B6a+c (2.19%)			
RB7	1-stem	B7a+b (99.28%)				
	2-stem		B7a,B7b (<1%)			
RB8	1-stem	B8a+b (99.25%)				
	2-stem		B8a,B8b (<1%)			
RB9	1-stem	B9a+b (95.50%)				
	2-stem		B9a+b (4.50%)			
RB10	1-stem		B10a+b,B10c (5.22%) B10a,B10b+c (66.09%) B10a+c,B10b (2.61%)	B10a,B10b,B10c (10.43%)		
	2-stem		B10a,B10b+c (15.65%) B10b,B10a+c (<1%)			

Table S13: Statistical analysis of diverse airway branching patterns of NLST-D59 dataset.

		Mono-	Bi-	Tri-	Quadri-
LUB B1-5			B1+2+3,B4+5 (92.42%)	B1+2+3,B4,B5 (2.47%)	
				B1+2,B3,B4+5 (5.11%)	
LLB B6-10				B6,B8+9,B10 (15.68%)	B6,B8,B9,B10 (9.16%)
				B6,B8,B9+10 (75.16%)	
LB1+2	1-stem		B1+2a+b,B1+2c (72.25%)	B1+2a,B1+2b,B1+2c (4.63%)	
			B1+2a,B1+2b+c (15.47%)		
			B1+2a+c,B1+2b (<1%)		
	2-stem		B1+2a+b,B1+2c (7.66%)		
			B1+2a,B1+2b+c (<1%)		
LB3	1-stem		B3a+b,B3c (8.53%)	B3a,B3b,B3c (9.04%)	
			B3a,B3b+c (76.11%)		
			B3a+c,B3b (<1%)		
	2-stem		B3a+b,B3c (1.37%)		
			B3a,B3b+c (4.95%)		
LB4	1-stem	B4a+b (89.38%)			
	2-stem		B4a,B4b (10.62%)		
LB5	1-stem	B5a+b (98.37%)			
	2-stem		B5a,B5b (1.63%)		
LB6	1-stem		B6a+b,B6c (41.11%)	B6a,B6b,B6c (22.82%)	
			B6a,B6b+c (29.53%)		
			B6a+c,B6b (6.38%)		
	2-stem		B6b,B6a+c (<1%)		
LB8	1-stem	B8a+b (97.69%)			
	2-stem		B8a,B8b (2.31%)		
LB9	1-stem	B9a+b (79.83%)			
	2-stem		B9a,B9b (20.17%)		
LB10	1-stem		B10a+b,B10c (1.08%)	B10a,B10b,B10c (10.22%)	
			B10a,B10b+c (73.66%)		
			B10a+c,B10b (12.90%)		
	2-stem		B10a,B10b+c (1.97%)		
			B10b,B10a+c (<1%)		

		Mono-	Bi-	Tri-	Quadri-	Quint-
RUB B1-3			B1+2,B3 (22.78%)	B1,B2,B3 (29.02%)		
			B1+3,B2 (18.56%)			
			B1,B2+3 (29.64%)			
RMB B4-5			B4,B5 (100%)			
RLB B6-10				B6,B8+9,B7+10 (<1%)	B6,B7,B8+9,B10 (19.01%)	B6,B7,B8,B9,B10 (23.03%)
					B6,B7,B8,B9+10 (57.95%)	
RB1	1-stem	B1a+b (90.60%)				
	2-stem		B1a,B1b (9.40%)			
RB2	1-stem	B2a+b (97.01%)				
	2-stem		B2a,B2b (2.99%)			
RB3	1-stem	B3a+b (94.26%)				
	2-stem		B3a,B3b (5.74%)			
RB4	1-stem	B4a+b (98.74%)				
	2-stem		B4a,B4b (1.26%)			
RB5	1-stem	B5a+b (92.99%)				
	2-stem		B5a,B5b (7.01%)			
RB6	1-stem		B6a+b,B6c (5.43%)	B6a,B6b,B6c (11.54%)		
			B6a,B6b+c (2.55%)			
			B6a+c,B6b (78.78%)			
	2-stem		B6a,B6b+c (<1%)			
			B6b,B6a+c (1.02%)			
RB7	1-stem	B7a+b (99.16%)				
	2-stem		B7a,B7b (<1%)			
RB8	1-stem	B8a+b (98.68%)				
	2-stem		B8a,B8b (1.32%)			
RB9	1-stem	B9a+b (92.86%)				
	2-stem		B9a+b (7.14%)			
RB10	1-stem		B10a+b,B10c (2.46%)	B10a,B10b,B10c (11.40%)		
			B10a,B10b+c (75.79%)			
			B10a+c,B10b (1.05%)			
	2-stem		B10a,B10b+c (9.30%)			
			B10b,B10a+c (<1%)			

Table S14: Statistical analysis of diverse airway branching patterns of NLST-D61 dataset.

		Mono-	Bi-	Tri-	Quadri-
LUB B1-5			B1+2+3,B4+5 (89.95%)	B1+2+3,B4,B5 (3.35%)	
				B1+2,B3,B4+5 (6.70%)	
LLB B6-10				B6,B8+9,B10 (17.33%)	B6,B8,B9,B10 (8.00%)
				B6,B8,B9+10 (74.67%)	
LB1+2	1-stem		B1+2a+b,B1+2c (68.71%)	B1+2a,B1+2b,B1+2c (6.12%)	
			B1+2a,B1+2b+c (15.42%)		
			B1+2a+c,B1+2b (<1%)		
	2-stem		B1+2a+b,B1+2c (9.07%)		
			B1+2a,B1+2b+c (<1%)		
LB3	1-stem		B3a+b,B3c (8.33%)	B3a,B3b,B3c (10.48%)	
			B3a,B3b+c (74.29%)		
			B3a+c,B3b (<1%)		
	2-stem		B3a+b,B3c (1.19%)		
			B3a,B3b+c (5.71%)		
LB4	1-stem	B4a+b (83.98%)			
	2-stem		B4a,B4b (16.02%)		
LB5	1-stem	B5a+b (98.97%)			
	2-stem		B5a,B5b (1.03%)		
LB6	1-stem		B6a+b,B6c (38.21%)	B6a,B6b,B6c (23.11%)	
			B6a,B6b+c (28.54%)		
			B6a+c,B6b (10.14%)		
	2-stem		B6b,B6a+c (<1%)		
LB8	1-stem	B8a+b (97.81%)			
	2-stem		B8a,B8b (2.19%)		
LB9	1-stem	B9a+b (86.63%)			
	2-stem		B9a,B9b (13.37%)		
LB10	1-stem		B10a+b,B10c (<1%)	B10a,B10b,B10c (9.25%)	
			B10a,B10b+c (70.80%)		
			B10a+c,B10b (15.82%)		
	2-stem		B10a,B10b+c (3.16%)		
			B10b,B10a+c (<1%)		

		Mono-	Bi-	Tri-	Quadri-	Quint-
RUB B1-3			B1+2,B3 (22.98%)	B1,B2,B3 (27.13%)		
			B1+3,B2 (23.19%)			
			B1,B2+3 (26.70%)			
RMB B4-5			B4,B5 (100%)			
RLB B6-10				B6,B8+9,B7+10 (<1%)	B6,B7,B8+9,B10 (18.81%)	B6,B7,B8,B9,B10 (25.00%)
					B6,B7,B8,B9+10 (56.19%)	
RB1	1-stem	B1a+b (91.39%)				
	2-stem		B1a,B1b (8.61%)			
RB2	1-stem	B2a+b (98.20%)				
	2-stem		B2a,B2b (1.80%)			
RB3	1-stem	B3a+b (94.97%)				
	2-stem		B3a,B3b (5.03%)			
RB4	1-stem	B4a+b (99.51%)				
	2-stem		B4a,B4b (<1%)			
RB5	1-stem	B5a+b (95.93%)				
	2-stem		B5a,B5b (4.07%)			
RB6	1-stem		B6a+b,B6c (6.09%)	B6a,B6b,B6c (8.67%)		
			B6a,B6b+c (2.58%)			
			B6a+c,B6b (81.26%)			
	2-stem		B6a,B6b+c (<1%)			
			B6b,B6a+c (1.17%)			
RB7	1-stem	B7a+b (98.82%)				
	2-stem		B7a,B7b (1.18%)			
RB8	1-stem	B8a+b (98.34%)				
	2-stem		B8a,B8b (1.66%)			
RB9	1-stem	B9a+b (94.37%)				
	2-stem		B9a+b (5.63%)			
RB10	1-stem		B10a+b,B10c (2.19%)	B10a,B10b,B10c (11.92%)		
			B10a,B10b+c (78.10%)			
			B10a+c,B10b (<1%)			
	2-stem		B10a,B10b+c (7.30%)			
			B10b,B10a+c (<1%)			

Table S15: The quantative morphological features of the AIIB23 group (experimental group).

	Health Control Group						AIIB23 Group					
Branch Name	Stenosis	Ectasia	Tortuosity	Divergence	Length	Complexity	Stenosis(p-value)	Ectasia(p-value)	Tortuosity(p-value)	Divergence(p-value)	Length(p-value)	Complexity(p-value)
LUB	0.27 ± 0.04	1.29 ± 0.03	0.64 ± 0.02	0.70 ± 0.05	45.33 ± 5.87	1.01 ± 0.06	0.27 ± 0.16(<0.01)	1.28 ± 0.25(<0.01)	0.60 ± 0.18(0.87)	0.63 ± 0.19(<0.01)	47.55 ± 9.98(0.13)	1.01 ± 0.13(<0.01)
LDB	0.29 ± 0.04	1.30 ± 0.03	0.65 ± 0.02	0.59 ± 0.07	49.70 ± 7.19	1.05 ± 0.08	0.30 ± 0.08(0.57)	1.32 ± 0.05(0.9)	0.62 ± 0.03(0.77)	0.59 ± 0.10(<0.01)	49.56 ± 9.42(0.68)	1.05 ± 0.10(<0.01)
RUB	0.27 ± 0.04	1.29 ± 0.03	0.64 ± 0.02	0.71 ± 0.08	45.26 ± 6.67	1.00 ± 0.07	0.27 ± 0.07(<0.01)	1.30 ± 0.05(<0.01)	0.61 ± 0.02(0.02)	0.67 ± 0.09(<0.01)	50.82 ± 8.00(0.63)	1.03 ± 0.09(0.04)
RMB	0.28 ± 0.05	1.29 ± 0.04	0.66 ± 0.03	0.36 ± 0.07	50.91 ± 7.58	0.87 ± 0.08	0.28 ± 0.07(<0.01)	1.30 ± 0.06(0.04)	0.63 ± 0.04(0.94)	0.33 ± 0.08(<0.01)	53.31 ± 9.11(0.81)	0.87 ± 0.09(0.19)
RDB	0.28 ± 0.04	1.29 ± 0.03	0.66 ± 0.02	0.70 ± 0.09	50.10 ± 6.24	1.09 ± 0.06	0.29 ± 0.08(<0.01)	1.32 ± 0.06(<0.01)	0.62 ± 0.03(<0.01)	0.64 ± 0.12(<0.01)	46.29 ± 7.93(0.23)	1.05 ± 0.10(<0.01)
LB1+2	0.28 ± 0.05	1.28 ± 0.04	0.64 ± 0.03	0.41 ± 0.08	47.31 ± 8.13	0.79 ± 0.09	0.27 ± 0.17(0.93)	1.27 ± 0.25(0.03)	0.60 ± 0.18(0.91)	0.39 ± 0.18(<0.01)	49.77 ± 12.39(0.23)	0.80 ± 0.13(0.03)
LB3	0.27 ± 0.05	1.29 ± 0.05	0.64 ± 0.03	0.49 ± 0.09	47.16 ± 6.15	0.79 ± 0.08	0.27 ± 0.16(<0.01)	1.28 ± 0.26(0.22)	0.59 ± 0.18(0.46)	0.43 ± 0.19(<0.01)	48.03 ± 11.26(0.04)	0.78 ± 0.13(0.01)
LB4	0.27 ± 0.06	1.30 ± 0.07	0.65 ± 0.04	0.37 ± 0.11	38.14 ± 7.30	0.63 ± 0.10	0.27 ± 0.22(<0.01)	1.27 ± 0.36(0.47)	0.58 ± 0.25(0.08)	0.27 ± 0.24(<0.01)	38.15 ± 12.29(0.04)	0.60 ± 0.17(<0.01)
LB5	0.33 ± 0.10	1.34 ± 0.13	0.67 ± 0.07	0.16 ± 0.11	43.40 ± 13.66	0.61 ± 0.12	0.30 ± 0.28(0.72)	1.30 ± 0.46(0.39)	0.59 ± 0.31(0.08)	0.12 ± 0.24(0.02)	40.11 ± 18.03(0.27)	0.57 ± 0.20(0.01)
LB6	0.27 ± 0.06	1.32 ± 0.15	0.62 ± 0.03	0.43 ± 0.09	39.23 ± 6.42	0.71 ± 0.09	0.29 ± 0.10(1)	1.34 ± 0.17(0.05)	0.60 ± 0.04(0.56)	0.43 ± 0.13(<0.01)	41.52 ± 9.57(0.21)	0.72 ± 0.14(0.3)
LB8	0.33 ± 0.12	1.31 ± 0.18	0.65 ± 0.13	0.30 ± 0.15	49.27 ± 12.29	0.71 ± 0.12	0.33 ± 0.10(<0.01)	1.33 ± 0.06(0.83)	0.63 ± 0.05(0.14)	0.36 ± 0.12(<0.01)	49.88 ± 13.19(0.47)	0.74 ± 0.14(0.34)
LB9	0.28 ± 0.14	1.29 ± 0.25	0.66 ± 0.17	0.27 ± 0.16	47.70 ± 12.69	0.69 ± 0.14	0.30 ± 0.09(0.99)	1.33 ± 0.07(0.78)	0.64 ± 0.05(0.24)	0.28 ± 0.11(<0.01)	47.75 ± 13.13(0.55)	0.71 ± 0.14(0.23)
LB10	0.30 ± 0.06	1.28 ± 0.04	0.65 ± 0.03	0.36 ± 0.10	57.44 ± 9.83	0.82 ± 0.09	0.29 ± 0.08(0.11)	1.31 ± 0.06(0.04)	0.62 ± 0.04(0.07)	0.33 ± 0.10(<0.01)	54.51 ± 11.39(0.68)	0.80 ± 0.11(<0.01)
RB1	0.29 ± 0.06	1.29 ± 0.04	0.63 ± 0.03	0.37 ± 0.12	43.88 ± 7.74	0.75 ± 0.09	0.28 ± 0.09(<0.01)	1.30 ± 0.06(<0.01)	0.61 ± 0.04(<0.01)	0.42 ± 0.12(<0.01)	50.24 ± 10.08(0.45)	0.80 ± 0.12(0.21)
RB2	0.27 ± 0.05	1.29 ± 0.05	0.64 ± 0.03	0.42 ± 0.09	40.88 ± 5.78	0.70 ± 0.08	0.28 ± 0.08(0.1)	1.31 ± 0.07(<0.01)	0.62 ± 0.04(0.08)	0.40 ± 0.10(<0.01)	43.79 ± 8.74(0.22)	0.72 ± 0.11(0.03)
RB3	0.26 ± 0.05	1.29 ± 0.07	0.65 ± 0.03	0.46 ± 0.09	48.99 ± 9.16	0.78 ± 0.10	0.27 ± 0.08(0.01)	1.30 ± 0.06(<0.01)	0.62 ± 0.03(<0.01)	0.43 ± 0.09(<0.01)	55.54 ± 9.25(0.34)	0.81 ± 0.10(0.26)
RB4	0.28 ± 0.05	1.29 ± 0.06	0.66 ± 0.04	0.28 ± 0.07	47.43 ± 8.04	0.72 ± 0.09	0.28 ± 0.09(0.13)	1.30 ± 0.07(0.85)	0.63 ± 0.04(0.09)	0.26 ± 0.11(<0.01)	47.67 ± 10.34(0.68)	0.69 ± 0.12(0.3)
RB5	0.29 ± 0.06	1.31 ± 0.07	0.66 ± 0.04	0.23 ± 0.07	53.31 ± 9.37	0.75 ± 0.10	0.30 ± 0.09(0.38)	1.33 ± 0.10(<0.01)	0.63 ± 0.05(0.58)	0.22 ± 0.10(<0.01)	57.45 ± 10.37(0.42)	0.76 ± 0.09(0.14)
RB6	0.26 ± 0.05	1.31 ± 0.08	0.63 ± 0.03	0.54 ± 0.10	40.39 ± 5.28	0.73 ± 0.08	0.28 ± 0.10(<0.01)	1.36 ± 0.20(0.81)	0.60 ± 0.04(0.31)	0.44 ± 0.15(<0.01)	40.65 ± 8.73(0.06)	0.71 ± 0.13(0.04)
RB7	0.21 ± 0.41	1.10 ± 0.73	0.48 ± 0.50	0.13 ± 0.40	38.37 ± 15.49	0.59 ± 0.22	0.27 ± 0.37(<0.01)	1.21 ± 0.63(0.07)	0.50 ± 0.42(0.79)	0.22 ± 0.36(<0.01)	37.46 ± 14.56(0.12)	0.58 ± 0.21(0.1)
RB8	0.30 ± 0.06	1.30 ± 0.06	0.68 ± 0.04	0.29 ± 0.10	53.62 ± 9.52	0.75 ± 0.09	0.29 ± 0.18(0.01)	1.30 ± 0.27(<0.01)	0.62 ± 0.19(<0.01)	0.24 ± 0.17(<0.01)	47.58 ± 12.54(0.94)	0.68 ± 0.14(0.03)
RB9	0.29 ± 0.06	1.31 ± 0.09	0.68 ± 0.05	0.24 ± 0.07	48.76 ± 10.63	0.68 ± 0.11	0.32 ± 0.11(<0.01)	1.34 ± 0.11(<0.01)	0.66 ± 0.06(0.01)	0.20 ± 0.09(0.03)	44.79 ± 11.14(0.03)	0.64 ± 0.15(<0.01)
RB10	0.28 ± 0.05	1.28 ± 0.04	0.66 ± 0.03	0.36 ± 0.08	58.25 ± 9.77	0.83 ± 0.09	0.30 ± 0.09(0.27)	1.31 ± 0.07(<0.01)	0.62 ± 0.04(<0.01)	0.35 ± 0.10(<0.01)	51.19 ± 10.33(0.23)	0.79 ± 0.11(<0.01)

Table S16: The quantative morphological features of the NLST-D54 group (experimental group).

	Health Control Group						NLST-D54 Group					
BranchName	Stenosis	Ectasia	Tortuosity	Divergence	Length	Complexity	Stenosis(p-value)	Ectasia(p-value)	Tortuosity(p-value)	Divergence(p-value)	Length(p-value)	Complexity(p-value)
LUB	0.27 ± 0.04	1.29 ± 0.03	0.64 ± 0.02	0.70 ± 0.05	45.33 ± 5.87	1.01 ± 0.06	0.22 ± 0.04(<0.01)	1.28 ± 0.04(0.03)	0.62 ± 0.02(<0.01)	0.68 ± 0.07(<0.01)	44.00 ± 7.13(<0.01)	0.93 ± 0.08(0.08)
LDB	0.29 ± 0.04	1.30 ± 0.03	0.65 ± 0.02	0.59 ± 0.07	49.70 ± 7.19	1.05 ± 0.08	0.24 ± 0.04(<0.01)	1.30 ± 0.04(<0.01)	0.62 ± 0.03(<0.01)	0.61 ± 0.08(<0.01)	44.23 ± 7.40(<0.01)	0.95 ± 0.10(0.94)
RUB	0.27 ± 0.04	1.29 ± 0.03	0.64 ± 0.02	0.71 ± 0.08	45.26 ± 6.67	1.00 ± 0.07	0.21 ± 0.04(<0.01)	1.27 ± 0.04(0.5)	0.62 ± 0.02(<0.01)	0.64 ± 0.09(<0.01)	44.83 ± 6.56(<0.01)	0.93 ± 0.07(<0.01)
RMB	0.28 ± 0.05	1.29 ± 0.04	0.66 ± 0.03	0.36 ± 0.07	50.91 ± 7.58	0.87 ± 0.08	0.25 ± 0.08(<0.01)	1.32 ± 0.11(<0.01)	0.61 ± 0.05(<0.01)	0.23 ± 0.08(<0.01)	37.70 ± 11.41(<0.01)	0.66 ± 0.20(<0.01)
RDB	0.28 ± 0.04	1.29 ± 0.03	0.66 ± 0.02	0.70 ± 0.09	50.10 ± 6.24	1.09 ± 0.06	0.24 ± 0.04(<0.01)	1.31 ± 0.04(<0.01)	0.63 ± 0.02(<0.01)	0.66 ± 0.11(<0.01)	43.91 ± 6.67(<0.01)	0.96 ± 0.08(<0.01)
LB1+2	0.28 ± 0.05	1.28 ± 0.04	0.64 ± 0.03	0.41 ± 0.08	47.31 ± 8.13	0.79 ± 0.09	0.21 ± 0.04(<0.01)	1.27 ± 0.07(<0.01)	0.64 ± 0.04(<0.01)	0.32 ± 0.09(0.52)	50.29 ± 9.00(<0.01)	0.73 ± 0.15(0.12)
LB3	0.27 ± 0.05	1.29 ± 0.05	0.64 ± 0.03	0.49 ± 0.09	47.16 ± 6.15	0.79 ± 0.08	0.21 ± 0.05(<0.01)	1.28 ± 0.07(<0.01)	0.61 ± 0.04(<0.01)	0.39 ± 0.12(<0.01)	43.16 ± 8.72(<0.01)	0.69 ± 0.17(0.49)
LB4	0.27 ± 0.06	1.30 ± 0.07	0.65 ± 0.04	0.37 ± 0.11	38.14 ± 7.30	0.63 ± 0.10	0.25 ± 0.09(<0.01)	1.33 ± 0.12(<0.01)	0.62 ± 0.07(<0.01)	0.26 ± 0.15(<0.01)	33.14 ± 11.82(<0.01)	0.47 ± 0.24(<0.01)
LB5	0.33 ± 0.10	1.34 ± 0.13	0.67 ± 0.07	0.16 ± 0.11	43.40 ± 13.66	0.61 ± 0.12	0.28 ± 0.10(0.12)	1.36 ± 0.16(<0.01)	0.63 ± 0.08(<0.01)	0.15 ± 0.12(<0.01)	34.21 ± 13.46(<0.01)	0.49 ± 0.19(0.07)
LB6	0.27 ± 0.06	1.32 ± 0.15	0.62 ± 0.03	0.43 ± 0.09	39.23 ± 6.42	0.71 ± 0.09	0.22 ± 0.06(0.59)	1.32 ± 0.11(<0.01)	0.59 ± 0.04(<0.01)	0.43 ± 0.11(<0.01)	36.37 ± 6.65(<0.01)	0.65 ± 0.11(0.81)
LB8	0.33 ± 0.12	1.31 ± 0.18	0.65 ± 0.13	0.30 ± 0.15	49.27 ± 12.29	0.71 ± 0.12	0.29 ± 0.08(0.38)	1.33 ± 0.10(<0.01)	0.62 ± 0.05(<0.01)	0.29 ± 0.13(<0.01)	42.43 ± 11.44(<0.01)	0.60 ± 0.17(0.26)
LB9	0.28 ± 0.14	1.29 ± 0.25	0.66 ± 0.17	0.27 ± 0.16	47.70 ± 12.69	0.69 ± 0.14	0.27 ± 0.09(<0.01)	1.33 ± 0.11(<0.01)	0.63 ± 0.06(<0.01)	0.26 ± 0.12(<0.01)	40.97 ± 11.88(<0.01)	0.58 ± 0.20(0.16)
LB10	0.30 ± 0.06	1.28 ± 0.04	0.65 ± 0.03	0.36 ± 0.10	57.44 ± 9.83	0.82 ± 0.09	0.23 ± 0.06(<0.01)	1.28 ± 0.06(<0.01)	0.64 ± 0.05(<0.01)	0.28 ± 0.11(<0.01)	54.55 ± 9.63(<0.01)	0.70 ± 0.17(0.87)
RB1	0.29 ± 0.06	1.29 ± 0.04	0.63 ± 0.03	0.37 ± 0.12	43.88 ± 7.74	0.75 ± 0.09	0.21 ± 0.04(0.3)	1.27 ± 0.06(<0.01)	0.64 ± 0.04(0.02)	0.36 ± 0.11(0.15)	47.45 ± 8.35(<0.01)	0.73 ± 0.12(<0.01)
RB2	0.27 ± 0.05	1.29 ± 0.05	0.64 ± 0.03	0.42 ± 0.09	40.88 ± 5.78	0.70 ± 0.08	0.23 ± 0.06(<0.01)	1.31 ± 0.12(<0.01)	0.61 ± 0.05(<0.01)	0.37 ± 0.11(<0.01)	38.61 ± 7.94(<0.01)	0.63 ± 0.17(0.08)
RB3	0.26 ± 0.05	1.29 ± 0.07	0.65 ± 0.03	0.46 ± 0.09	48.99 ± 9.16	0.78 ± 0.10	0.21 ± 0.06(<0.01)	1.27 ± 0.07(<0.01)	0.60 ± 0.04(<0.01)	0.37 ± 0.10(<0.01)	45.31 ± 9.62(<0.01)	0.68 ± 0.17(<0.01)
RB4	0.28 ± 0.05	1.29 ± 0.06	0.66 ± 0.04	0.28 ± 0.07	47.43 ± 8.04	0.72 ± 0.09	0.26 ± 0.08(<0.01)	1.34 ± 0.14(<0.01)	0.61 ± 0.05(<0.01)	0.21 ± 0.10(<0.01)	35.27 ± 10.24(<0.01)	0.47 ± 0.25(<0.01)
RB5	0.29 ± 0.06	1.31 ± 0.07	0.66 ± 0.04	0.23 ± 0.07	53.31 ± 9.37	0.75 ± 0.10	0.24 ± 0.08(<0.01)	1.30 ± 0.09(<0.01)	0.62 ± 0.05(<0.01)	0.20 ± 0.10(<0.01)	41.32 ± 12.81(<0.01)	0.51 ± 0.27(0.21)
RB6	0.26 ± 0.05	1.31 ± 0.08	0.63 ± 0.03	0.54 ± 0.10	40.39 ± 5.28	0.73 ± 0.08	0.22 ± 0.05(<0.01)	1.32 ± 0.08(<0.01)	0.60 ± 0.04(<0.01)	0.41 ± 0.10(<0.01)	35.33 ± 6.50(<0.01)	0.63 ± 0.13(0.25)
RB7	0.21 ± 0.41	1.10 ± 0.73	0.48 ± 0.50	0.13 ± 0.40	38.37 ± 15.49	0.59 ± 0.22	0.29 ± 0.07(0.02)	1.36 ± 0.16(0.78)	0.65 ± 0.05(0.08)	0.24 ± 0.10(0.24)	43.09 ± 9.82(<0.01)	0.55 ± 0.20(0.12)
RB8	0.30 ± 0.06	1.30 ± 0.06	0.68 ± 0.04	0.29 ± 0.10	53.62 ± 9.52	0.75 ± 0.09	0.27 ± 0.09(<0.01)	1.33 ± 0.13(<0.01)	0.63 ± 0.06(<0.01)	0.22 ± 0.10(<0.01)	42.53 ± 10.98(<0.01)	0.55 ± 0.23(<0.01)
RB9	0.29 ± 0.06	1.31 ± 0.09	0.68 ± 0.05	0.24 ± 0.07	48.76 ± 10.63	0.68 ± 0.11	0.29 ± 0.10(<0.01)	1.39 ± 0.21(<0.01)	0.65 ± 0.08(<0.01)	0.18 ± 0.11(<0.01)	40.35 ± 12.32(0.51)	0.52 ± 0.22(<0.01)
RB10	0.28 ± 0.05	1.28 ± 0.04	0.66 ± 0.03	0.36 ± 0.08	58.25 ± 9.77	0.83 ± 0.09	0.23 ± 0.05(<0.01)	1.30 ± 0.12(<0.01)	0.65 ± 0.05(<0.01)	0.29 ± 0.09(0.04)	51.69 ± 9.81(<0.01)	0.71 ± 0.18(<0.01)

Table S17: The quantative morphological features of the NLST-D58 group (experimental group).

	Health Control Group						NLST-D58 Group					
BranchName	Stenosis	Ectasia	Tortuosity	Divergence	Length	Complexity	Stenosis(p-value)	Ectasia(p-value)	Tortuosity(p-value)	Divergence(p-value)	Length(p-value)	Complexity(p-value)
LUB	0.27 ± 0.04	1.29 ± 0.03	0.64 ± 0.02	0.70 ± 0.05	45.33 ± 5.87	1.01 ± 0.06	0.22 ± 0.04(0.01)	1.28 ± 0.04(0.01)	0.62 ± 0.02(<0.01)	0.68 ± 0.08(<0.01)	43.70 ± 6.78(<0.01)	0.92 ± 0.08(0.23)
LDB	0.29 ± 0.04	1.30 ± 0.03	0.65 ± 0.02	0.59 ± 0.07	49.70 ± 7.19	1.05 ± 0.08	0.25 ± 0.04(0.13)	1.30 ± 0.04(<0.01)	0.62 ± 0.03(<0.01)	0.60 ± 0.11(<0.01)	45.44 ± 7.40(<0.01)	0.94 ± 0.09(0.09)
RUB	0.27 ± 0.04	1.29 ± 0.03	0.64 ± 0.02	0.71 ± 0.08	45.26 ± 6.67	1.00 ± 0.07	0.22 ± 0.03(<0.01)	1.28 ± 0.04(0.02)	0.61 ± 0.02(<0.01)	0.61 ± 0.10(<0.01)	43.60 ± 6.69(<0.01)	0.91 ± 0.08(0.03)
RMB	0.28 ± 0.05	1.29 ± 0.04	0.66 ± 0.03	0.36 ± 0.07	50.91 ± 7.58	0.87 ± 0.08	0.26 ± 0.07(<0.01)	1.32 ± 0.09(<0.01)	0.61 ± 0.05(<0.01)	0.22 ± 0.08(<0.01)	35.65 ± 11.57(<0.01)	0.60 ± 0.24(<0.01)
RDB	0.28 ± 0.04	1.29 ± 0.03	0.66 ± 0.02	0.70 ± 0.09	50.10 ± 6.24	1.09 ± 0.06	0.25 ± 0.04(<0.01)	1.32 ± 0.04(<0.01)	0.63 ± 0.03(<0.01)	0.66 ± 0.11(<0.01)	43.71 ± 7.62(<0.01)	0.94 ± 0.09(<0.01)
LB1+2	0.28 ± 0.05	1.28 ± 0.04	0.64 ± 0.03	0.41 ± 0.08	47.31 ± 8.13	0.79 ± 0.09	0.22 ± 0.05(<0.01)	1.27 ± 0.06(<0.01)	0.64 ± 0.04(<0.01)	0.30 ± 0.09(0.18)	51.09 ± 10.33(<0.01)	0.73 ± 0.11(0.27)
LB3	0.27 ± 0.05	1.29 ± 0.05	0.64 ± 0.03	0.49 ± 0.09	47.16 ± 6.15	0.79 ± 0.08	0.22 ± 0.05(<0.01)	1.28 ± 0.07(<0.01)	0.61 ± 0.04(<0.01)	0.38 ± 0.12(<0.01)	41.99 ± 7.24(<0.01)	0.66 ± 0.18(0.23)
LB4	0.27 ± 0.06	1.30 ± 0.07	0.65 ± 0.04	0.37 ± 0.11	38.14 ± 7.30	0.63 ± 0.10	0.26 ± 0.09(<0.01)	1.34 ± 0.12(<0.01)	0.61 ± 0.07(<0.01)	0.25 ± 0.14(<0.01)	29.80 ± 10.77(0.12)	0.44 ± 0.23(<0.01)
LB5	0.33 ± 0.10	1.34 ± 0.13	0.67 ± 0.07	0.16 ± 0.11	43.40 ± 13.66	0.61 ± 0.12	0.28 ± 0.10(0.02)	1.36 ± 0.16(<0.01)	0.64 ± 0.08(<0.01)	0.14 ± 0.10(<0.01)	36.38 ± 19.09(<0.01)	0.48 ± 0.21(0.24)
LB6	0.27 ± 0.06	1.32 ± 0.15	0.62 ± 0.03	0.43 ± 0.09	39.23 ± 6.42	0.71 ± 0.09	0.23 ± 0.06(0.3)	1.34 ± 0.13(<0.01)	0.60 ± 0.04(<0.01)	0.44 ± 0.12(<0.01)	37.07 ± 7.73(<0.01)	0.62 ± 0.15(0.21)
LB8	0.33 ± 0.12	1.31 ± 0.18	0.65 ± 0.13	0.30 ± 0.15	49.27 ± 12.29	0.71 ± 0.12	0.31 ± 0.08(<0.01)	1.34 ± 0.11(<0.01)	0.63 ± 0.05(<0.01)	0.27 ± 0.12(<0.01)	44.16 ± 10.79(<0.01)	0.63 ± 0.12(0.04)
LB9	0.28 ± 0.14	1.29 ± 0.25	0.66 ± 0.17	0.27 ± 0.16	47.70 ± 12.69	0.69 ± 0.14	0.28 ± 0.09(0.02)	1.34 ± 0.11(<0.01)	0.63 ± 0.07(<0.01)	0.25 ± 0.12(<0.01)	41.37 ± 13.15(0.19)	0.56 ± 0.21(0.05)
LB10	0.30 ± 0.06	1.28 ± 0.04	0.65 ± 0.03	0.36 ± 0.10	57.44 ± 9.83	0.82 ± 0.09	0.24 ± 0.06(<0.01)	1.28 ± 0.05(0.06)	0.65 ± 0.04(<0.01)	0.28 ± 0.11(0.03)	55.53 ± 9.32(<0.01)	0.70 ± 0.18(0.76)
RB1	0.29 ± 0.06	1.29 ± 0.04	0.63 ± 0.03	0.37 ± 0.12	43.88 ± 7.74	0.75 ± 0.09	0.22 ± 0.05(0.01)	1.27 ± 0.05(<0.01)	0.64 ± 0.04(<0.01)	0.35 ± 0.10(0.23)	47.12 ± 8.51(<0.01)	0.72 ± 0.10(0.01)
RB2	0.27 ± 0.05	1.29 ± 0.05	0.64 ± 0.03	0.42 ± 0.09	40.88 ± 5.78	0.70 ± 0.08	0.24 ± 0.06(<0.01)	1.31 ± 0.09(0.02)	0.61 ± 0.05(<0.01)	0.37 ± 0.12(<0.01)	39.06 ± 7.80(<0.01)	0.59 ± 0.22(0.03)
RB3	0.26 ± 0.05	1.29 ± 0.07	0.65 ± 0.03	0.46 ± 0.09	48.99 ± 9.16	0.78 ± 0.10	0.22 ± 0.06(<0.01)	1.29 ± 0.08(<0.01)	0.59 ± 0.04(<0.01)	0.36 ± 0.12(<0.01)	42.43 ± 10.10(<0.01)	0.63 ± 0.20(0.75)
RB4	0.28 ± 0.05	1.29 ± 0.06	0.66 ± 0.04	0.28 ± 0.07	47.43 ± 8.04	0.72 ± 0.09	0.27 ± 0.09(<0.01)	1.32 ± 0.12(<0.01)	0.61 ± 0.06(<0.01)	0.22 ± 0.10(<0.01)	34.23 ± 10.87(0.27)	0.41 ± 0.28(<0.01)
RB5	0.29 ± 0.06	1.31 ± 0.07	0.66 ± 0.04	0.23 ± 0.07	53.31 ± 9.37	0.75 ± 0.10	0.26 ± 0.07(<0.01)	1.33 ± 0.13(<0.01)	0.62 ± 0.06(<0.01)	0.20 ± 0.10(<0.01)	39.05 ± 12.15(<0.01)	0.45 ± 0.29(0.08)
RB6	0.26 ± 0.05	1.31 ± 0.08	0.63 ± 0.03	0.54 ± 0.10	40.39 ± 5.28	0.73 ± 0.08	0.23 ± 0.06(<0.01)	1.34 ± 0.10(<0.01)	0.59 ± 0.04(<0.01)	0.39 ± 0.11(<0.01)	34.58 ± 7.24(<0.01)	0.61 ± 0.14(<0.01)
RB7	0.21 ± 0.41	1.10 ± 0.73	0.48 ± 0.50	0.13 ± 0.40	38.37 ± 15.49	0.59 ± 0.22	0.30 ± 0.08(<0.01)	1.35 ± 0.17(0.49)	0.65 ± 0.06(<0.01)	0.22 ± 0.10(0.08)	43.58 ± 10.69(<0.01)	0.53 ± 0.21(0.46)
RB8	0.30 ± 0.06	1.30 ± 0.06	0.68 ± 0.04	0.29 ± 0.10	53.62 ± 9.52	0.75 ± 0.09	0.29 ± 0.08(<0.01)	1.34 ± 0.13(<0.01)	0.63 ± 0.07(<0.01)	0.23 ± 0.12(<0.01)	42.70 ± 11.00(0.02)	0.53 ± 0.24(<0.01)
RB9	0.29 ± 0.06	1.31 ± 0.09	0.68 ± 0.05	0.24 ± 0.07	48.76 ± 10.63	0.68 ± 0.11	0.31 ± 0.11(<0.01)	1.40 ± 0.19(<0.01)	0.65 ± 0.09(<0.01)	0.15 ± 0.10(<0.01)	40.92 ± 14.45(0.1)	0.51 ± 0.22(<0.01)
RB10	0.28 ± 0.05	1.28 ± 0.04	0.66 ± 0.03	0.36 ± 0.08	58.25 ± 9.77	0.83 ± 0.09	0.25 ± 0.06(<0.01)	1.31 ± 0.08(<0.01)	0.65 ± 0.05(<0.01)	0.27 ± 0.09(0.09)	51.74 ± 10.97(<0.01)	0.70 ± 0.17(<0.01)

Table S18: The quantative morphological features of the NLST-D59 group (experimental group).

	Health Control Group						NLST-D59 Group					
BranchName	Stenosis	Ectasia	Tortuosity	Divergence	Length	Complexity	Stenosis(p-value)	Ectasia(p-value)	Tortuosity(p-value)	Divergence(p-value)	Length(p-value)	Complexity(p-value)
LUB	0.27 ± 0.04	1.29 ± 0.03	0.64 ± 0.02	0.70 ± 0.05	45.33 ± 5.87	1.01 ± 0.06	0.21 ± 0.03(0.02)	1.27 ± 0.03(0.09)	0.63 ± 0.02(<0.01)	0.71 ± 0.07(<0.01)	46.20 ± 7.34(<0.01)	0.97 ± 0.09(<0.01)
LDB	0.29 ± 0.04	1.30 ± 0.03	0.65 ± 0.02	0.59 ± 0.07	49.70 ± 7.19	1.05 ± 0.08	0.23 ± 0.04(<0.01)	1.29 ± 0.04(<0.01)	0.64 ± 0.03(<0.01)	0.63 ± 0.08(<0.01)	47.87 ± 8.18(<0.01)	1.00 ± 0.10(<0.01)
RUB	0.27 ± 0.04	1.29 ± 0.03	0.64 ± 0.02	0.71 ± 0.08	45.26 ± 6.67	1.00 ± 0.07	0.20 ± 0.03(<0.01)	1.27 ± 0.04(0.03)	0.62 ± 0.02(<0.01)	0.66 ± 0.10(<0.01)	46.46 ± 7.58(<0.01)	0.97 ± 0.10(<0.01)
RMB	0.28 ± 0.05	1.29 ± 0.04	0.66 ± 0.03	0.36 ± 0.07	50.91 ± 7.58	0.87 ± 0.08	0.24 ± 0.07(<0.01)	1.30 ± 0.08(<0.01)	0.63 ± 0.04(<0.01)	0.27 ± 0.08(<0.01)	41.76 ± 10.99(<0.01)	0.73 ± 0.20(0.98)
RDB	0.28 ± 0.04	1.29 ± 0.03	0.66 ± 0.02	0.70 ± 0.09	50.10 ± 6.24	1.09 ± 0.06	0.23 ± 0.04(<0.01)	1.29 ± 0.04(<0.01)	0.64 ± 0.03(<0.01)	0.68 ± 0.11(<0.01)	46.46 ± 7.66(<0.01)	1.01 ± 0.10(0.52)
LB1+2	0.28 ± 0.05	1.28 ± 0.04	0.64 ± 0.03	0.41 ± 0.08	47.31 ± 8.13	0.79 ± 0.09	0.20 ± 0.04(<0.01)	1.26 ± 0.05(<0.01)	0.65 ± 0.04(<0.01)	0.33 ± 0.09(0.01)	52.64 ± 9.30(<0.01)	0.76 ± 0.11(<0.01)
LB3	0.27 ± 0.05	1.29 ± 0.05	0.64 ± 0.03	0.49 ± 0.09	47.16 ± 6.15	0.79 ± 0.08	0.20 ± 0.04(<0.01)	1.27 ± 0.06(<0.01)	0.62 ± 0.04(<0.01)	0.44 ± 0.12(<0.01)	45.55 ± 8.94(<0.01)	0.74 ± 0.16(<0.01)
LB4	0.27 ± 0.06	1.30 ± 0.07	0.65 ± 0.04	0.37 ± 0.11	38.14 ± 7.30	0.63 ± 0.10	0.24 ± 0.08(<0.01)	1.31 ± 0.11(<0.01)	0.62 ± 0.06(<0.01)	0.29 ± 0.14(<0.01)	35.40 ± 10.36(<0.01)	0.56 ± 0.19(0.2)
LB5	0.33 ± 0.10	1.34 ± 0.13	0.67 ± 0.07	0.16 ± 0.11	43.40 ± 13.66	0.61 ± 0.12	0.25 ± 0.09(0.97)	1.33 ± 0.15(<0.01)	0.65 ± 0.07(<0.01)	0.16 ± 0.10(<0.01)	39.69 ± 12.72(<0.01)	0.57 ± 0.16(0.3)
LB6	0.27 ± 0.06	1.32 ± 0.15	0.62 ± 0.03	0.43 ± 0.09	39.23 ± 6.42	0.71 ± 0.09	0.21 ± 0.05(<0.01)	1.31 ± 0.09(0.83)	0.61 ± 0.04(0.01)	0.46 ± 0.10(<0.01)	39.12 ± 7.47(<0.01)	0.69 ± 0.12(0.14)
LB8	0.33 ± 0.12	1.31 ± 0.18	0.65 ± 0.13	0.30 ± 0.15	49.27 ± 12.29	0.71 ± 0.12	0.28 ± 0.07(0.79)	1.32 ± 0.10(0.15)	0.64 ± 0.05(<0.01)	0.30 ± 0.12(<0.01)	48.16 ± 11.62(<0.01)	0.68 ± 0.15(0.55)
LB9	0.28 ± 0.14	1.29 ± 0.25	0.66 ± 0.17	0.27 ± 0.16	47.70 ± 12.69	0.69 ± 0.14	0.25 ± 0.07(0.17)	1.31 ± 0.10(<0.01)	0.64 ± 0.05(<0.01)	0.29 ± 0.12(<0.01)	44.94 ± 11.90(<0.01)	0.65 ± 0.18(0.55)
LB10	0.30 ± 0.06	1.28 ± 0.04	0.65 ± 0.03	0.36 ± 0.10	57.44 ± 9.83	0.82 ± 0.09	0.22 ± 0.05(<0.01)	1.27 ± 0.05(0.49)	0.65 ± 0.04(<0.01)	0.31 ± 0.10(0.45)	56.89 ± 10.27(<0.01)	0.76 ± 0.14(<0.01)
RB1	0.29 ± 0.06	1.29 ± 0.04	0.63 ± 0.03	0.37 ± 0.12	43.88 ± 7.74	0.75 ± 0.09	0.20 ± 0.04(0.53)	1.27 ± 0.05(<0.01)	0.64 ± 0.04(0.57)	0.37 ± 0.12(<0.01)	48.73 ± 8.68(<0.01)	0.76 ± 0.11(<0.01)
RB2	0.27 ± 0.05	1.29 ± 0.05	0.64 ± 0.03	0.42 ± 0.09	40.88 ± 5.78	0.70 ± 0.08	0.21 ± 0.05(<0.01)	1.29 ± 0.08(0.95)	0.62 ± 0.04(<0.01)	0.38 ± 0.11(<0.01)	40.84 ± 8.41(<0.01)	0.66 ± 0.17(0.3)
RB3	0.26 ± 0.05	1.29 ± 0.07	0.65 ± 0.03	0.46 ± 0.09	48.99 ± 9.16	0.78 ± 0.10	0.20 ± 0.05(<0.01)	1.27 ± 0.05(0.02)	0.61 ± 0.04(<0.01)	0.41 ± 0.10(<0.01)	47.16 ± 9.87(<0.01)	0.73 ± 0.18(<0.01)
RB4	0.28 ± 0.05	1.29 ± 0.06	0.66 ± 0.04	0.28 ± 0.07	47.43 ± 8.04	0.72 ± 0.09	0.24 ± 0.07(<0.01)	1.30 ± 0.11(<0.01)	0.64 ± 0.05(<0.01)	0.23 ± 0.09(<0.01)	40.18 ± 10.28(<0.01)	0.56 ± 0.24(0.03)
RB5	0.29 ± 0.06	1.31 ± 0.07	0.66 ± 0.04	0.23 ± 0.07	53.31 ± 9.37	0.75 ± 0.10	0.23 ± 0.07(<0.01)	1.29 ± 0.08(<0.01)	0.63 ± 0.05(<0.01)	0.20 ± 0.08(<0.01)	45.00 ± 11.71(<0.01)	0.59 ± 0.25(<0.01)
RB6	0.26 ± 0.05	1.31 ± 0.08	0.63 ± 0.03	0.54 ± 0.10	40.39 ± 5.28	0.73 ± 0.08	0.21 ± 0.05(<0.01)	1.31 ± 0.08(<0.01)	0.60 ± 0.04(<0.01)	0.46 ± 0.12(<0.01)	38.16 ± 7.14(<0.01)	0.68 ± 0.14(0.41)
RB7	0.21 ± 0.41	1.10 ± 0.73	0.48 ± 0.50	0.13 ± 0.40	38.37 ± 15.49	0.59 ± 0.22	0.27 ± 0.07(<0.01)	1.36 ± 0.21(<0.01)	0.66 ± 0.05(0.87)	0.23 ± 0.10(<0.01)	44.83 ± 10.43(<0.01)	0.58 ± 0.19(0.09)
RB8	0.30 ± 0.06	1.30 ± 0.06	0.68 ± 0.04	0.29 ± 0.10	53.62 ± 9.52	0.75 ± 0.09	0.26 ± 0.07(<0.01)	1.31 ± 0.10(<0.01)	0.65 ± 0.05(<0.01)	0.24 ± 0.10(<0.01)	47.31 ± 11.39(<0.01)	0.63 ± 0.21(0.06)
RB9	0.29 ± 0.06	1.31 ± 0.09	0.68 ± 0.05	0.24 ± 0.07	48.76 ± 10.63	0.68 ± 0.11	0.27 ± 0.09(<0.01)	1.35 ± 0.17(<0.01)	0.66 ± 0.07(<0.01)	0.20 ± 0.10(<0.01)	42.85 ± 12.76(<0.01)	0.58 ± 0.20(<0.01)
RB10	0.28 ± 0.05	1.28 ± 0.04	0.66 ± 0.03	0.36 ± 0.08	58.25 ± 9.77	0.83 ± 0.09	0.22 ± 0.05(<0.01)	1.28 ± 0.06(<0.01)	0.65 ± 0.04(<0.01)	0.31 ± 0.09(0.26)	53.92 ± 10.26(<0.01)	0.76 ± 0.15(0.74)

Table S19: The quantative morphological features of the NLST-D61 group (experimental group).

	Health Control Group						NLST-D61 Group					
BranchName	Stenosis	Ectasia	Tortuosity	Divergence	Length	Complexity	Stenosis(p-value)	Ectasia(p-value)	Tortuosity(p-value)	Divergence(p-value)	Length(p-value)	Complexity(p-value)
LUB	0.27 ± 0.04	1.29 ± 0.03	0.64 ± 0.02	0.70 ± 0.05	45.33 ± 5.87	1.01 ± 0.06	0.21 ± 0.03(0.28)	1.27 ± 0.03(0.93)	0.63 ± 0.02(<0.01)	0.70 ± 0.07(<0.01)	45.28 ± 6.96(<0.01)	0.97 ± 0.08(<0.01)
LDB	0.29 ± 0.04	1.30 ± 0.03	0.65 ± 0.02	0.59 ± 0.07	49.70 ± 7.19	1.05 ± 0.08	0.23 ± 0.04(<0.01)	1.28 ± 0.04(<0.01)	0.63 ± 0.03(<0.01)	0.63 ± 0.09(<0.01)	47.38 ± 8.10(<0.01)	1.00 ± 0.09(<0.01)
RUB	0.27 ± 0.04	1.29 ± 0.03	0.64 ± 0.02	0.71 ± 0.08	45.26 ± 6.67	1.00 ± 0.07	0.20 ± 0.03(<0.01)	1.27 ± 0.04(0.2)	0.62 ± 0.02(<0.01)	0.66 ± 0.10(<0.01)	46.00 ± 7.20(<0.01)	0.97 ± 0.10(<0.01)
RMB	0.28 ± 0.05	1.29 ± 0.04	0.66 ± 0.03	0.36 ± 0.07	50.91 ± 7.58	0.87 ± 0.08	0.24 ± 0.07(<0.01)	1.29 ± 0.07(<0.01)	0.63 ± 0.04(<0.01)	0.27 ± 0.09(<0.01)	42.01 ± 10.95(<0.01)	0.74 ± 0.19(0.63)
RDB	0.28 ± 0.04	1.29 ± 0.03	0.66 ± 0.02	0.70 ± 0.09	50.10 ± 6.24	1.09 ± 0.06	0.23 ± 0.04(0.02)	1.29 ± 0.04(<0.01)	0.64 ± 0.02(<0.01)	0.68 ± 0.12(<0.01)	45.88 ± 7.53(<0.01)	1.01 ± 0.09(0.62)
LB1+2	0.28 ± 0.05	1.28 ± 0.04	0.64 ± 0.03	0.41 ± 0.08	47.31 ± 8.13	0.79 ± 0.09	0.20 ± 0.04(<0.01)	1.26 ± 0.05(<0.01)	0.64 ± 0.04(<0.01)	0.33 ± 0.09(0.48)	51.47 ± 9.34(<0.01)	0.76 ± 0.11(<0.01)
LB3	0.27 ± 0.05	1.29 ± 0.05	0.64 ± 0.03	0.49 ± 0.09	47.16 ± 6.15	0.79 ± 0.08	0.20 ± 0.05(<0.01)	1.27 ± 0.06(<0.01)	0.62 ± 0.03(<0.01)	0.44 ± 0.12(<0.01)	44.49 ± 8.54(<0.01)	0.74 ± 0.15(<0.01)
LB4	0.27 ± 0.06	1.30 ± 0.07	0.65 ± 0.04	0.37 ± 0.11	38.14 ± 7.30	0.63 ± 0.10	0.23 ± 0.08(<0.01)	1.30 ± 0.10(<0.01)	0.62 ± 0.06(<0.01)	0.31 ± 0.14(<0.01)	34.67 ± 9.82(<0.01)	0.55 ± 0.21(0.39)
LB5	0.33 ± 0.10	1.34 ± 0.13	0.67 ± 0.07	0.16 ± 0.11	43.40 ± 13.66	0.61 ± 0.12	0.25 ± 0.09(0.83)	1.32 ± 0.13(<0.01)	0.64 ± 0.07(<0.01)	0.17 ± 0.10(<0.01)	38.28 ± 11.45(<0.01)	0.56 ± 0.17(0.09)
LB6	0.27 ± 0.06	1.32 ± 0.15	0.62 ± 0.03	0.43 ± 0.09	39.23 ± 6.42	0.71 ± 0.09	0.20 ± 0.05(<0.01)	1.30 ± 0.08(0.36)	0.61 ± 0.04(0.01)	0.46 ± 0.10(<0.01)	38.71 ± 7.54(<0.01)	0.68 ± 0.13(0.02)
LB8	0.33 ± 0.12	1.31 ± 0.18	0.65 ± 0.13	0.30 ± 0.15	49.27 ± 12.29	0.71 ± 0.12	0.28 ± 0.07(0.67)	1.31 ± 0.10(<0.01)	0.64 ± 0.05(<0.01)	0.31 ± 0.12(<0.01)	46.91 ± 11.30(<0.01)	0.67 ± 0.16(0.19)
LB9	0.28 ± 0.14	1.29 ± 0.25	0.66 ± 0.17	0.27 ± 0.16	47.70 ± 12.69	0.69 ± 0.14	0.26 ± 0.08(0.5)	1.32 ± 0.11(<0.01)	0.65 ± 0.06(<0.01)	0.29 ± 0.12(<0.01)	44.19 ± 11.93(<0.01)	0.65 ± 0.17(0.82)
LB10	0.30 ± 0.06	1.28 ± 0.04	0.65 ± 0.03	0.36 ± 0.10	57.44 ± 9.83	0.82 ± 0.09	0.22 ± 0.05(<0.01)	1.27 ± 0.05(0.41)	0.65 ± 0.04(<0.01)	0.31 ± 0.10(0.01)	56.74 ± 10.57(<0.01)	0.76 ± 0.13(<0.01)
RB1	0.29 ± 0.06	1.29 ± 0.04	0.63 ± 0.03	0.37 ± 0.12	43.88 ± 7.74	0.75 ± 0.09	0.20 ± 0.04(0.49)	1.27 ± 0.05(<0.01)	0.64 ± 0.03(0.86)	0.37 ± 0.11(0.02)	48.30 ± 8.46(<0.01)	0.75 ± 0.11(<0.01)
RB2	0.27 ± 0.05	1.29 ± 0.05	0.64 ± 0.03	0.42 ± 0.09	40.88 ± 5.78	0.70 ± 0.08	0.21 ± 0.05(<0.01)	1.29 ± 0.09(0.42)	0.62 ± 0.04(<0.01)	0.38 ± 0.11(<0.01)	40.43 ± 7.84(<0.01)	0.66 ± 0.16(0.69)
RB3	0.26 ± 0.05	1.29 ± 0.07	0.65 ± 0.03	0.46 ± 0.09	48.99 ± 9.16	0.78 ± 0.10	0.20 ± 0.05(<0.01)	1.26 ± 0.06(<0.01)	0.61 ± 0.03(<0.01)	0.42 ± 0.11(<0.01)	46.45 ± 9.00(<0.01)	0.73 ± 0.17(<0.01)
RB4	0.28 ± 0.05	1.29 ± 0.06	0.66 ± 0.04	0.28 ± 0.07	47.43 ± 8.04	0.72 ± 0.09	0.25 ± 0.08(<0.01)	1.30 ± 0.10(<0.01)	0.63 ± 0.05(<0.01)	0.24 ± 0.09(<0.01)	39.64 ± 10.07(<0.01)	0.57 ± 0.23(0.18)
RB5	0.29 ± 0.06	1.31 ± 0.07	0.66 ± 0.04	0.23 ± 0.07	53.31 ± 9.37	0.75 ± 0.10	0.23 ± 0.07(<0.01)	1.29 ± 0.08(<0.01)	0.63 ± 0.05(<0.01)	0.21 ± 0.09(<0.01)	45.85 ± 11.40(<0.01)	0.61 ± 0.24(<0.01)
RB6	0.26 ± 0.05	1.31 ± 0.08	0.63 ± 0.03	0.54 ± 0.10	40.39 ± 5.28	0.73 ± 0.08	0.21 ± 0.05(<0.01)	1.31 ± 0.09(<0.01)	0.60 ± 0.03(<0.01)	0.46 ± 0.12(<0.01)	37.72 ± 6.95(<0.01)	0.68 ± 0.14(0.36)
RB7	0.21 ± 0.41	1.10 ± 0.73	0.48 ± 0.50	0.13 ± 0.40	38.37 ± 15.49	0.59 ± 0.22	0.28 ± 0.07(<0.01)	1.34 ± 0.16(0.03)	0.66 ± 0.05(0.84)	0.23 ± 0.09(<0.01)	44.59 ± 10.45(<0.01)	0.58 ± 0.19(0.77)
RB8	0.30 ± 0.06	1.30 ± 0.06	0.68 ± 0.04	0.29 ± 0.10	53.62 ± 9.52	0.75 ± 0.09	0.26 ± 0.08(<0.01)	1.31 ± 0.10(<0.01)	0.65 ± 0.06(<0.01)	0.24 ± 0.11(<0.01)	45.96 ± 11.38(<0.01)	0.63 ± 0.20(0.02)
RB9	0.29 ± 0.06	1.31 ± 0.09	0.68 ± 0.05	0.24 ± 0.07	48.76 ± 10.63	0.68 ± 0.11	0.27 ± 0.09(<0.01)	1.35 ± 0.17(<0.01)	0.65 ± 0.07(<0.01)	0.20 ± 0.10(<0.01)	41.84 ± 12.47(<0.01)	0.57 ± 0.20(<0.01)
RB10	0.28 ± 0.05	1.28 ± 0.04	0.66 ± 0.03	0.36 ± 0.08	58.25 ± 9.77	0.83 ± 0.09	0.22 ± 0.05(<0.01)	1.28 ± 0.06(<0.01)	0.65 ± 0.04(<0.01)	0.31 ± 0.09(0.05)	53.06 ± 9.47(<0.01)	0.77 ± 0.11(0.49)